Solid solution chemistry of geothermally-deposited calcite:
Fluid-mineral equilibria applications

Timothy J. Callahan

submitted in partial fulfillment of the degree Master of Science, Geochemistry

Department of Earth and Environmental Science

New Mexico Institute of Mining and Technology

August, 1995

ABSTRACT

The chemical relationship between calcite samples and their parent fluids is investigated here by measuring the concentrations of Cu^{2+}, Pb^{2+}, Zn^{2+}, Mg^{2+}, and Fe^{2+} in calcite and parent fluid samples. The objective of this study is to use recent theoretical data concerning carbonate mineral solubility products and Henry's Law constants to calculate the chemistry of the unknown end member if only one end member is available for analysis; for example, the chemistry of the parent fluid can be estimated by analyzing calcite left behind. This has direct applications to ore deposits in which calcite is cogenetic with ore minerals and where certain general chemical conditions can be gathered from fluid inclusions in the minerals.

The systems studied here involved only those from which both calcite and parent fluid samples could be obtained. This allowed us to gauge the pertinence of the theoretical data to real depositing systems. The data show a general correlation between the measured and calculated chemistry, especially for the calcite samples collected from a hydrothermal ore deposit, likely due to accurate chemical analysis of fluid inclusions from the calcite and other cogenetic minerals.

Overall, theoretical solubility products and Henry's Law constants successfully allow the calculation of water composition from our analyzed calcite data. As the experimental data improves for ligand formation constants and activity coefficients of aqueous species, the accuracy of solid solution chemistry calculations will improve as well. For systems in which the general fluid chemistry is known or can be estimated, analysis of calcite could quantitatively determine divalent cation composition of the paleofluid.

ACKNOWLEDGEMENTS

Many thanks to David Norman and Robert Smith for their interest in this research, and who supported this thesis work from the beginning. Carl Popp and Peter Mozley also receive much-deserved appreciation for their guidance during my thesis studies. Barbara Popp, Lynn Brandvold, Sandy Swartz, and the entire chemical laboratory staff at the New Mexico Institute Bureau of Mines and Mineral Resources are recognized for their succor and support during the laboratory work, as well as those scientists who generously provided sample materials and without whom the research would not have been possible.

Laboratory research was also supported by the New Mexico Tech Graduate Student Research Project Scholarships, the Anita and Antonius Budding Award, and the Barkley Wycoff Memorial Scholarship; the author would like to acknowledge the above benefactors for their generosity.

The camaraderie and companionship I enjoyed at New Mexico Tech with the many people I met during my stay in Socorro made graduate school life more bearable; for this, I am grateful. I would especially like to thank Brad Yonaka and Charlie Ferranti for lending insightful advice and editorial assistance in (sometime frantic) times of need. Lastly, I am indebted to Rita Lam for her patience, grace, and understanding; always.

TABLE OF CONTENTS

TABLE OF CONTENTS (continued)

LIST OF FIGURES

FIGURE Page

Background

Methods

Results

Discussion

LIST OF TABLES

TABLE Page

Background

Methods

Results

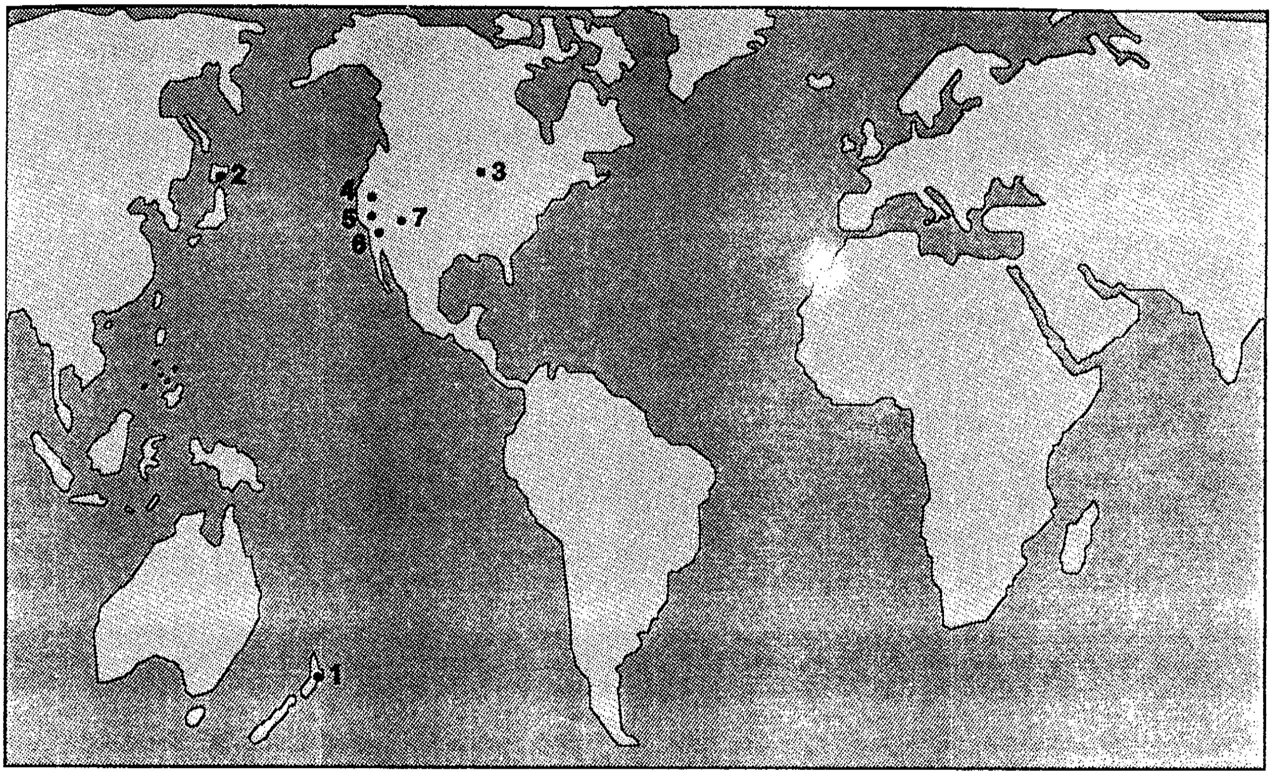

1. Broadlands/Ohaaki, New Zealand
2. Nigorikawa, Hokkaido, Japan
3. Tribag Mine, Ontario
4. Dixie Valley, Nevada
5. Coso Hydrothermal Field, China Lake, California
6. Salton Sea, Imperial Valley, California
7. Valles Caldera, Jemez Mountains, New Mexico

Plate 1. Sample location map.

INTRODUCTION

By studying calcite and the water from which it precipitated, a chemical correlation between the two can be achieved. Calcite has low levels of various divalent cations in its crystal lattice, due to substitution of like-size cations for Ca^{2+}. The concentration of each metal in solid solution with calcite is a function of the chemical activity of the metals in both the solid and the depositing solution. Theoretically, it is possible to predict the concentration of divalent cations in the depositing solutions knowing the concentration of the cations in the calcite. For this prediction to be valid, equilibrium conditions between the calcite and the depositing solution must exist. Variables affecting the distribution of a cation between calcite and the depositing solution are: solution temperature, salinity of the water, concentration of complexing anions in solution (such as Cl^-, HS^-), and complexation constants for the particular cation with these anions.

Calcite samples collected from eight geothermal fields, one ore deposit, and one vein system were analyzed for low levels (≤ 1 ppm) of Cu, Pb, Zn, Mg, Fe, and Mn. Recent theoretical data concerning solid solution chemistry allows us to use these analyses to calculate metal concentrations in the depositing fluid. The relationship between a fluid and the minerals it deposits under equilibrium conditions is influenced heavily by thermodynamics at high temperatures (> 200°C), and by kinetics at lower temperatures (Morse and Bender, 1990). The mineral-depositing systems found at geothermal fields were examined in this study, because calcite is frequently deposited and water chemistry data is readily available. Therefore, theoretical data can be checked for validity in real mineral-depositing situations.

We compared the analyzed and calculated compositions of calcite and the water from which it was deposited. This was done by using Henry's Law constants and solubility products to estimate the composition of water from calcite analytical data. Similarly, manipulation of analytical water data provided theoretical calcite compositions. Generally, the data shows a fair comparison between the analytical and calculated values. Ideally, the calculated and the analyzed values should be the same, yet in some cases, substantial differences exist. To calculate one end member using analytical data from the other, certain chemical conditions must be known, e.g., the temperature of the water at time of deposition, the salinity of the water, and the concentration of metal-complexing ligands. The best data were collected for calcite from depositing systems in which the chemical conditions were well known (e.g., Tribag, Ontario;

Broadlands, New Zealand; Nigorikawa, Japan). Ambiguous information for some of the other samples may be the cause of the discrepancy between the analyzed and calculated data.

These results can be applied to mineral deposits in which calcite is cogenetic with ore minerals. Estimations of deposition temperature and fluid salinity are obtainable from fluid inclusion measurements; therefore, solid solution chemistry theory can quantitatively calculate the concentration of certain metals in the paleofluid.

BACKGROUND

Previously, there have only been a few ways to gauge the characteristics of an ancient mineral-depositing water by studying the minerals left behind. Fluid inclusions in minerals can give an estimate of the formation temperature for the minerals, as well as the salinity of the solution(s) in question (Roedder, 1984). Measurement of isotope ratios in minerals provides information on the source of mineral-depositing solutions (Ohmoto, 1979). Yet there has been no quantitative way to calculate the actual chemistry of mineral-depositing solutions. Recent data for solubility products and Henry's Law constants provide theoretical insight on carbonate solid solution chemistry (Smith and Jenne, in press). These data are employed to investigate the relationships between calcite and the solution from which it has been deposited.

Solid solution relationships

In the following section, the background theory is presented for solid solution relationships between a liquid and calcite with which it may be in chemical equilibrium. The copper (II) ion is used in as an example of trace level substitution of a divalent metal in calcite.

Substitution of divalent metals for calcium in calcite

Recent data has been released concerning the solid solution equilibrium constants (K) for calcite and certain divalent cations (Table 1; Smith and Jenne, in press). The data list solubility products for divalent cations as carbonate species; for example,

$$\mathbf{CaCO_3 \Leftrightarrow Ca^{2+} + CO_3^{2-}} \qquad (1),$$

$$\mathbf{Cu^{2+} + CO_3^{2-} \Leftrightarrow CuCO_3} \qquad (2).$$

Adding equations 1 and 2 gives the solid-solution relationship for copper carbonate and calcium carbonate:

$$\mathbf{[CaCO_3]_{ss} + Cu^{2+}_{aq} \Leftrightarrow [CuCO_3]_{ss} + Ca^{2+}_{aq}} \qquad (3),$$

The solubility products are represented by the general equations:

Table 1. Log solubility products for rhombohedral carbonate minerals (from Smith and Jenne, in press).

Species		**100° C**	**150**	**200**	**250**	**300**
$CaCO_3$	log K	-9.32	-10.11	-11.08	-12.26	-13.72
$CuCO_3$	log K	-10.50	-11.26	-12.19	-13.33	-14.74
$PbCO_3$	log K	-10.73	-11.04	-11.62	-12.49	-13.68
$ZnCO_3$	log K	-10.88	-11.73	-12.74	-13.95	-15.43
$MnCO_3$	log K	-11.47	-12.11	-12.95	-14.03	-15.38
$FeCO_3$	log K	-11.50	-12.36	-13.37	-14.59	-16.07
$MgCO_3$	log K	-9.92	-10.93	-12.05	-13.35	-14.89

$$\mathbf{K_1 = (a_{Ca^{2+}}\, a_{CO_3^{2-}})/a_{CaCO_3}} \qquad (4),$$

$$\mathbf{K_2 = a_{CuCO_3}/(a_{Cu^{2+}}\, a_{CO_3^{2-}})} \qquad (5),$$

where a_{CuCO_3} and a_{CaCO_3} are the activities of copper and calcium carbonate, $a_{Cu^{2+}}$ and $a_{Ca^{2+}}$ refer to copper and calcium in the aqueous phase, and $a_{CO_3^{2-}}$ is the activity of the carbonate ion.

For a fluid-mineral system in equilibrium, solid solution between calcite and divalent cations in solution can be represented by equation 3; a small proportion of Cu^{2+} can substitute for Ca^{2+} in calcite (Appelo and Postma, 1993). The solubility product for equation 3 ($K_3 = K_1 \cdot K_2$) is:

$$\mathbf{K_3 = (a_{Ca^{2+}}/a_{Cu^{2+}})(a_{CuCO_3}/a_{CaCO_3})} \qquad (6).$$

The activity of a species is equal to the product of its concentration (m = moles/kg) and activity coefficient (γ), or:

$$\mathbf{a_i = m_i \gamma_i} \qquad (7).$$

The extended Debye-Hückel equation is one way to estimate the activity coefficient of a dissolved species.

$$\mathbf{-\log \gamma_i = [A z_i^2 I^{1/2}]/[1 + å_i B I^{1/2}] + bI} \qquad (8).$$

This equation requires information on the amount of dissolved species in solution, or ionic strength (I); A, B, b, and $å_i$ are constants dependent on temperature and the ion in question. Using this knowledge, the software program ION is employed here to calculate the activity coefficients using the Debye-Hückel equation. Activity coefficients used for this study are listed in Table 2. The activity of neutral species in dilute waters is assumed to be unity; however, this is an invalid assumption at higher salinity (Brimhall and Crerar, 1987; McKibben and Williams, 1991; Wood, 1991). The ionic strength of a solution is a determination of the average electric field around an ion in solution,

$$\mathbf{I = \tfrac{1}{2}\Sigma m_i z_i^2} \qquad (9).$$

For most geothermal solutions, the ionic strength can be determined by adding the products of concentration and charge for the major cations, specifically, sodium and potassium (Henley, et al., 1984). Equation 6 can now be written as:

$$\mathbf{K_3 = (m_{Ca^{2+}}/m_{Cu^{2+}})(\gamma_{Ca^{2+}}/\gamma_{Cu^{2+}})(a_{CuCO_3}/a_{CaCO_3})} \qquad (10),$$

Table 2. Activity coefficients used in this study, calculated from ION, except where noted

sample	I[1]	γ_{M}[2]	γ_{Pb}	γ_{Mg}	γ_{Cl}	γ_{MCl_n}[3]	γ_{PbCl_n}	γ_{MgCl_n}
DV	0.016	0.428	0.407	0.454	0.791	0.798	0.795	0.808
COSO 8	0.023	0.264	0.241	0.295	0.687	0.700	0.693	0.716
COSO 20	0.047	0.181	0.155	0.216	0.607	0.626	0.616	0.651
NT302	0.100	0.205	0.171	0.248	0.616	0.639	0.628	0.669
BR11	0.034	0.268	0.241	0.303	0.686	0.700	0.693	0.719
TBG	0.405	0.040	0.023	0.069	0.336	0.381	0.359	0.439
VC2B	0.100	0.132	0.104	0.170	0.538	0.565	0.551	0.600
SSDP	3.0	0.015	0.005	0.034	0.179	0.231	0.206	0.298

[1] ionic strength of solution [2] activity coefficient for Cu, Zn, Mn, Fe, Ca

[3] activity coefficient for chloride complex for the above cations, where n = 1 or 3

where $m_{Ca^{2+}}$, $m_{Cu^{2+}}$, $\gamma_{Ca^{2+}}$, and $\gamma_{Cu^{2+}}$ list the concentration and activity coefficients of calcium and copper in solution, and m_{CuCO_3}, and m_{CaCO_3} denote the concentration and activity coefficient of calcium carbonate and copper carbonate in the calcite phase. The activity of $CaCO_3$ in calcite is assumed to be unity, therefore equation 11 can be simplified:

$$\mathbf{K_3 = (a_{CuCO_3})(m_{Ca^{2+}}/m_{Cu^{2+}})(\gamma_{Ca^{2+}}/\gamma_{Cu^{2+}})} \qquad \textbf{(11).}$$

The constant K in equation 11 is an apparent distribution constant (Tsusue and Holland, 1966), since cations form complexes with ligands (such as chloride, bisulfide, and hydroxide) in solution:

$$\mathbf{k = (a_{CuCO_3})(m_{Ca^{2+}}/m_{Cu(tot)})(\gamma_{Ca^{2+}}/\gamma_{Cu^{2+}})} \qquad \textbf{(12).}$$

The concentration of copper, $m_{Cu(tot)}$, is the sum of $m_{Cu^{2+}}$ plus any metal complexes in solution, such as $CuCl^+$, $CuCl_2$, $CuCl_3^-$, $Cu(HS)_2$, $Cu(HS)_3^-$, and $Cu(OH)^+$. Copper forms complexes with the chloride ion as follows:

$$\mathbf{CuCl^+ \Leftrightarrow Cu^{2+} + Cl^-} \qquad \textbf{(13),}$$

$$\mathbf{CuCl_2 \Leftrightarrow Cu^{2+} + 2Cl^-} \qquad \textbf{(14),}$$

$$\mathbf{CuCl_3^- \Leftrightarrow Cu^{2+} + 3Cl^-} \qquad \textbf{(15).}$$

The cumulative formation constants (Table 3) for the above reactions are:

$$\beta_1 = \mathbf{[a_{Cu^{2+}}\, a_{Cl^-}]/a_{CuCl^+}} \qquad \textbf{(16),}$$

$$\beta_2 = \mathbf{[a_{Cu^{2+}}(a_{Cl^-})^2]/a_{CuCl_2}} \qquad \textbf{(17),}$$

$$\beta_3 = \mathbf{[a_{Cu^{2+}}\,(a_{Cl^-})^3]/a_{CuCl_3^-}} \qquad \textbf{(18).}$$

Complexation with other ligands are represented similarly (Table 4). Therefore, $m_{Cu^{2+}}$ is only a fraction of the total copper concentration in solution, and is related to $m_{Cu(tot)}$ by the relationship (Tsusue and Holland, 1966):

$$\mathbf{m_{Cu^{2+}} = (m_{Cu(tot)})/(1 + \alpha)} \qquad \textbf{(19),}$$

where α is

$$\alpha = [\gamma_{Cu^{2+}}\,(\gamma_{Cl^-}\,\mathbf{m}_{Cl^-})]/(\beta_1\,\gamma_{CuCl^+}) + [\gamma_{Cu^{2+}}\,(\gamma_{Cl^-}\,\mathbf{m}_{Cl^-})^2]/(\beta_2\,\gamma_{CuCl_2}) + \cdots \qquad \textbf{(20).}$$

Equation 12 can now be arranged to solve for the activity of $CuCO_3$ in calcite:

$$\mathbf{a_{CuCO_3} = [(m_{Cu^{2+}}/m_{Ca^{2+}})(\gamma_{Cu^{2+}}/\gamma_{Ca^{2+}})]K_3} \qquad \textbf{(21).}$$

The activity of a mineral species in solid solution with calcite is related to concentration

Table 3. Cumulative formation constants for divalent cations and the chloride ion.

$MCl_n^{2-n} = M^{2+} + nCl^-$			Temperature (°C)		
Sources	element	log B_n	200	250	300
Helgeson (1969)	Cu	n = 1	-3.7	-4.8	-6
		2	-3.7	-4.9	-6.5
		3	-3.1	-4.6	-6.5
Bourcier and Barnes (1987)	Zn	1	-3.14	-4.35	-5.65
		2	-4.27	-5.64	-7.22
		3	-5.21	-6.68	-8.1
Seward (1984)	Pb	1	-2.55	-3.18	-3.89
		2	-4.00	-4.98	-6.26
		3	-3.81	-5.03	-6.76
Bourcier and Barnes (1987)	Mg	n = 1	-1.88	-2.24	-2.59
		2	(-3.0)[1]	(-3.9)	(-5.1)
		3	(-3.7)	(-4.9)	(-6.0)
Heinrich and Seward (1990)	Fe	1	n.d.	-3.78	-5.12
		2	n.d.	(-4.5)	(-5.7)
		3	n.d.	(-5.7)	(-6.7)
Williams-Jones and Seward (1989)	Ca	1	-0.50	-1.13	-2.20
		2	-0.94	-2.48	-3.48
		3	n.d.	-2.6	-4.0

[1] Values in parentheses are extrapolated and may be in error of up to 0.5 log units.
n.d.: no data.

Table 4. Formation constants for zinc and the bisulfide (HS^-) ion.

$ZnS + H_2S + HS^- = Zn(HS)_3^-$		log K		
Source	element	200°C	250	300
Bourcier and Barnes (1987)	Zn	-3.1	-3.2	-3.4

through Henry's Law:

$$a_{CuCO_3} = X_{CuCO_3} K_H \qquad (22),$$

where X_{CuCO_3} is the mole fraction of copper carbonate in solid solution with calcite and K_H is the Henry's Law coefficient (Table 5).

Henry's Law constants for carbonate species have been theoretically determined (Smith and Jenne, in press). From these data, the mole fraction of a divalent cation can be estimated. Therefore, the fraction of copper in calcite can be found by:

$$\%Cu_{cal} = (MM_{Cu}X_{CuCO_3})/[MM_{Ca}(1-X_{CuCO_3}) + MM_{Cu}X_{CuCO_3} + MM_{CO_3}] \times 100 \qquad (23),$$

where $\%Cu_{cal}$ is the percent copper in calcite; MM refers to the molar mass of a particular species; and X_{CuCO_3} is the mole fraction of copper carbonate in solid solution with calcite (equation 22).

The preceding equations can predict the amount of copper in calcite deposited by a fluid under equilibrium conditions. To make such a prediction, the temperature, ionic strength, and concentrations of calcium, chloride, and the metals in question must be known or estimated. Conversely, these equations can also be used to estimate the concentration of certain divalent cations in a paleofluid using measured data from calcite. Therefore, using measured data from calcite, the mole fraction of copper carbonate in solid solution with calcite (X_{CuCO_3}) can be calculated:

$$X_{CuCO_3} = \%Cu_{cal}(MM_{Ca} + MM_{CO_3})/(MM_{Cu}(1+\%Cu_{cal}) - \%Cu_{cal}MM_{Ca}) \qquad (24).$$

Equations 19 through 24 can be used in the reverse order to determine the amount of copper in the calcite-depositing solution ($m_{Cu(tot)}$).

In order to use the above equations, certain chemical conditions must be known. This information may be accessible through fluid inclusion measurements, obtained from calcite samples deposited at a relatively constant temperature. Inclusions in calcite give homogenization temperatures for the inclusions, which are estimates of the temperature during inclusion formation. These estimates may represent the deposition, or equilibrium, temperature of formation for that particular sample of calcite. Ionic strength, chloride, and perhaps calcium concentration can be estimated from salinity measurements of the inclusions as well.

In this study, calcite samples from geothermal fields were used because water chemistry data is available for these fields, and calcite is deposited at high temperatures. Using calcite

Table 5. Practical Henry's Law constants for divalent cation substitution into calcite (modified from Smith and Jenne, in press).

Species	**constant**	**100° C**	**150**	**200**	**250**	**300**
$CuCO_3$	K_H	130	100	81	66	54
$PbCO_3$	K_H	14	12	11	10	8.8
$ZnCO_3$	K_H	100	83	67	55	46
$MnCO_3$	K_H	7.4	6.7	6.1	5.6	5.1
$FeCO_3$	K_H	31	26	23	19	17
$MgCO_3$	K_H	160	130	100	81	66

chemistry data, theoretically-determined Henry's Law constants and solubility products are checked for pertinence to real situations. However, this practical application of theoretical data is invalid if the water chemistry data collected at geothermal fields are not genetically related to the calcite deposited, or if the calcite has been altered after deposition by waters of different chemistry.

Atomic absorption spectrophotometry

Calcite samples were measured using atomic absorption spectrophotometry (AA). Price (1972) and Hartley, et al. (1980) give adequate descriptions of atomic absorption theory. A general, practical summary is listed here, adapted from Hartley, et al. (1980). AA follows the Beer-Lambert-Bouguer Law in that a beam of a certain intensity (I) and wavelength (λ) is attenuated through a flame produced by a mixture of combustible gases, usually a combination of two gases such as air and acetylene, or acetylene and N_2O. The degree of attenuation depends on the absorption of such emitted beam,

$$\mathbf{I = I_o e^{-KL}} \qquad \mathbf{(25),}$$

where I is the intensity of the emergent beam; I_o is the emitted beam; K is a factor dependent on the wavelength of the beam, temperature, and concentration of the fluid; and L is the path length of the flame. On a logarithmic scale, I/I_o is proportional to the concentration of the particular element to be measured:

$$\mathbf{\log (I/I_o) = e\ c\ L} \qquad \mathbf{(26),}$$

where e represents the molar absorptivity and c is the concentration of the element in the fluid. The expression log (I/I_o) is also known as the absorbance, A. Absorbance is inversely related to transmittance (T), by:

$$\mathbf{A = -\log T} \qquad \mathbf{(27).}$$

Flame method

There are two types of atomic absorption spectrometry, flame and graphite furnace atomization. In the flame method, transmittance of the beam through a flame of either an acetylene/air mix or a mixture of acetylene and nitrous oxide (N_2O) gases can be used, depending on the cation analyzed. Fluid atomizes in the flame, and the beam transmitted through that flame is correlated to concentration of an element in the sample. This being the case, high levels of dissolved solids in the samples may cause anomalous attenuation of the transmitted beam. Therefore, comparing samples and standards of a different matrix may give erroneous data.

An Allied® atomic absorption/emission (flame) spectrophotometer, located at the New Mexico Bureau of Mines and Mineral Resources, New Mexico Tech, was used for analyses (Fig. 1). Detection of copper, lead, zinc, iron, and manganese required an acetylene-air flame, whereas magnesium and calcium were measured using a N_2O-acetylene flame. Because only one element can be measured at a time, single element standards were used. Each element was measured as a specific wavelength (Table 6). Standards were prepared by diluting Fisher Scientific AA Standards (1000 ppm) with 2% HNO_3 or HCl in distilled, deionized water (Table 7).

Graphite furnace method

The flame and graphite furnace methods employ different atomization techniques of the liquid sample (Beaty, 1978). The flame method measures the atomized sample in the steady state; i.e., the sample applied to the flame is constant. In the graphite furnace method, only a few microliters of sample are applied to the furnace, which are then atomized completely. This provides a temporary absorption signal, resulting in an absorbance peak. This peak depends on the absolute weight of the element introduced, unlike the flame method, where absorbance is relative to concentration in the liquid sample.

In the graphite furnace method, an electric arc vaporizes the liquid sample in a graphite crucible at high temperatures (Blackburn and Dennen, 1988). This is a more sensitive method of analysis than the flame method.

A Varian® atomic absorption spectrometer was used to analyze samples for copper and lead levels less than the flame method detection limit. Although the amount of calcium in the samples was lessened using the IEX procedure, it was necessary to dilute the samples 1:1 with Milli-Q Type 1 ($>$18.2 meg ohms) distilled, deionized water to further decrease the amount of calcium. The graphite furnace AA analytical method has lower detection limits than the flame method.

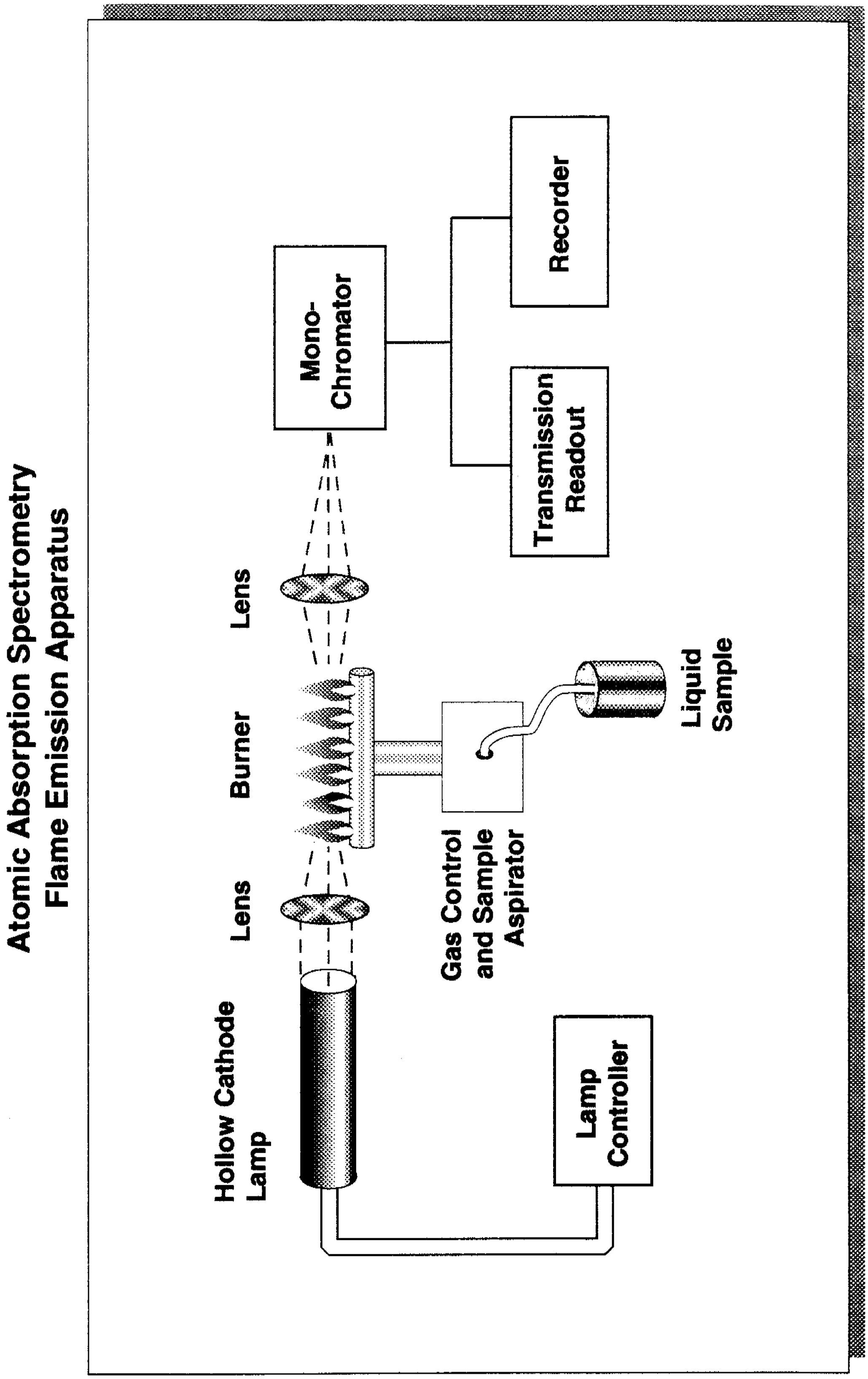

Figure 1. Illustration of the atomic absorption spectrophotometry technique, modified from Blackburn and Dennen (1988).

Table 6. Wavelength spectra for flame AA analysis.

Element	Mg	Pb	Zn	Cu	Fe	Mn
Wavelength (nm)	202.5	217.0	213.9	324.7	386.0	403.1

Table 7. Detection limits, atomic absorption spectrometry.

Element	flame method (ppb)	graphite furnace (ppb)
Pb	100	0.20
Cu	50	0.20
Zn	30	0.01
Mn	200	n.d.
Mg	500	n.d.
Fe	500	0.20

n.d.: no data

METHODS

Various laboratory methods were adapted or developed for this study; for example, calcite sample cleaning was done following the procedures of Roedder (1984). Also, the acid digestion technique was perfected as the laboratory work progressed, and eventually the final solution weight for each sample was decreased in order to maximize the cation concentrations in solution. Initial calcite analysis using atomic absorption spectrophotometry was conducted according to traditional flame AA procedures (Brandvold, 1994). However, laboratory techniques for ion exchange chromatography were adapted from previous work (Horwitz, et al., 1993) to increase the accuracy of low-level measurements of cations in saline solutions.

Calcite sample preparation

The calcite samples (see Appendix A for descriptions) were first crushed using a porcelain mortar and pestle to less than 0.5 mm size. Next, they were hand picked to remove non-calcite phases. The samples were put in a stainless steel flask with distilled, deionized water and the flask was then placed in an ultrasonic bath for about one hour. Next, they were transferred to an electrolytic cleaning system, which consisted of glass U-shaped tubes with electrodes at each end (Roedder. 1984). They remained in the cells up to 5 hours, the water being changed every hour. Samples were removed from the cells and then dried overnight.

Analytical techniques

Depositing waters

Data for the calcite-depositing waters were obtained either from published sources or from atomic absorption spectrometry analysis. The water data from Nigorikawa, Japan and Broadlands/Ohaaki, New Zealand were listed as discharge (surface) composition. The downhole compositions for these samples were calculated as follows (Henley, et al., 1984):

$$\mathbf{C_D = C_F \times (1\text{-}y)} \qquad \mathbf{(28),}$$

where C_D is the concentration of an aqueous species downhole, C_F is the concentration after flashing (steam loss), and y is the steam fraction of the initial fluid. The steam fraction is determined by:

$$\mathbf{y = (H_{L(T°C)} - H_{L(100°C)})/H_E} \qquad \mathbf{(29),}$$

where $H_{L(T°C)}$ represents the enthalpy of water at the downhole temperature, $H_{L(100°C)}$ is the enthalpy of water after steam loss, and H_E is the evaporation enthalpy of water.

The water chemistry data published for the other samples were assumed to be the best representation of downhole conditions. Some systems lacked adequate chemistry data; for these samples, the water data used for this study really only served as an estimation.

For the samples from Coso Junction and Dixie Valley, water collected at the surface of these geothermal systems was analyzed via AA for Ca, Cu, Pb, Zn, Mg, Fe, and Mn. Chloride and downhole temperature data were obtained from either published reports (Benoit 1989) or from personal communications (Moore, 1994).

Calcite samples

Most samples were split in half and each measured separately to determine analytical precision. Each split weighed between 2 to 10 grams. Calcite was dissolved by formic acid (HCOOH), mixed with three parts Milli-Q Type 1 (> 18.2 meg ohms) distilled, deionized water, then filtered through 100 ml Nalgene® cellulose filters (< 0.45 μm pore size). Each filter was flushed with eight filter volumes of Type 1 water before filtering the samples. A small residue of amorphous phases remained after every sample was filtered; the weight of solids remaining on the filter was subtracted from the sample weight to obtain the total amount of calcite dissolved.

Initial analyses

Fifteen samples from various geothermal fields, after being dissolved in acid, were analyzed for Cu, Pb, Zn, Mg, Fe and Mn by means of atomic absorption spectrometry (AA). Analytical errors resulted because of the high levels of dissolved calcium in the samples. The analyses implied two separate problems; the samples indicated much higher concentrations of metals than predicted by theoretical calculation, and the samples taken from separate locations all registered similar values for the metals (Table 8). The similar values obtained from the different calcite samples suggest analytical error resulting from the high concentrations of calcium in the solutions.

Attempts to measure trace metals in calcium-rich solutions

Since the analyses by direct measurement of dissolved calcite were suspect, several attempts were made to avoid the problem of high calcium levels in the samples. First, samples were measured against standards having high calcium concentrations. Normally, standards for atomic absorption spectrometry (AA) calibration are prepared from 1000 ppm solutions diluted to a range of concentrations in dilute acid (either HNO_3 or HCl). Standards were prepared for each element in a (5%) calcium matrix to approximate the solutions obtained by dissolving $CaCO_3$; this resulted in severe loss of detection sensitivity for metals. For example, lead could not be detected in solutions at concentrations less than 10 ppm. Analyses of zinc, manganese, copper, iron, and to a lesser degree, magnesium were also affected by calcium in solution. In addition, calcium-rich solutions caused mechanical problems with the atomizer and burner head of the spectrophotometer.

Standards were prepared to investigate the effects of matrix interference that occur during AA analysis of trace metals in Ca-rich solutions. In one test, six metals were measured, all in a matrix of 1% calcium (Fig. 2). Most noteworthy is the large error at low (0.1 ppm) metal concentrations. Another test checked the precision of metal analysis at varying calcium concentrations by measuring the cation concentrations in solutions of varying calcium content. This was done to find the detection limits of trace metals verses concentration of calcium in solution (Fig. 3 and 4). The results indicated that reliable detection of metals at concentrations less than 0.05 ppm is only possible in solutions that have 500 ppm or less calcium. Hence, it was deemed necessary to reduce the amount of calcium in the samples before analysis.

To this end, ion exchange chromatography (IEX) was used to separate the metal cations from calcium.

Table 8. Comparison of measured amounts of metals in geothermal calcite to values calculated from the chemistry and temperature of the waters.

Sample	NT 302[2]	SSDP[3]
indicated Pb in calcite (ppm[1])	51.45	53.59
calculated Pb in calcite (ppm)	2.29	20411
measured Pb in depositing water (ppm)	n.d.	95.0
calculated Pb in depositing water based on indicated Pb in calcite (ppm)	n.d.	0.25

[1] parts per million

[2] Nigorikawa, Japan

[3] Salton, CA

n.d.: no data

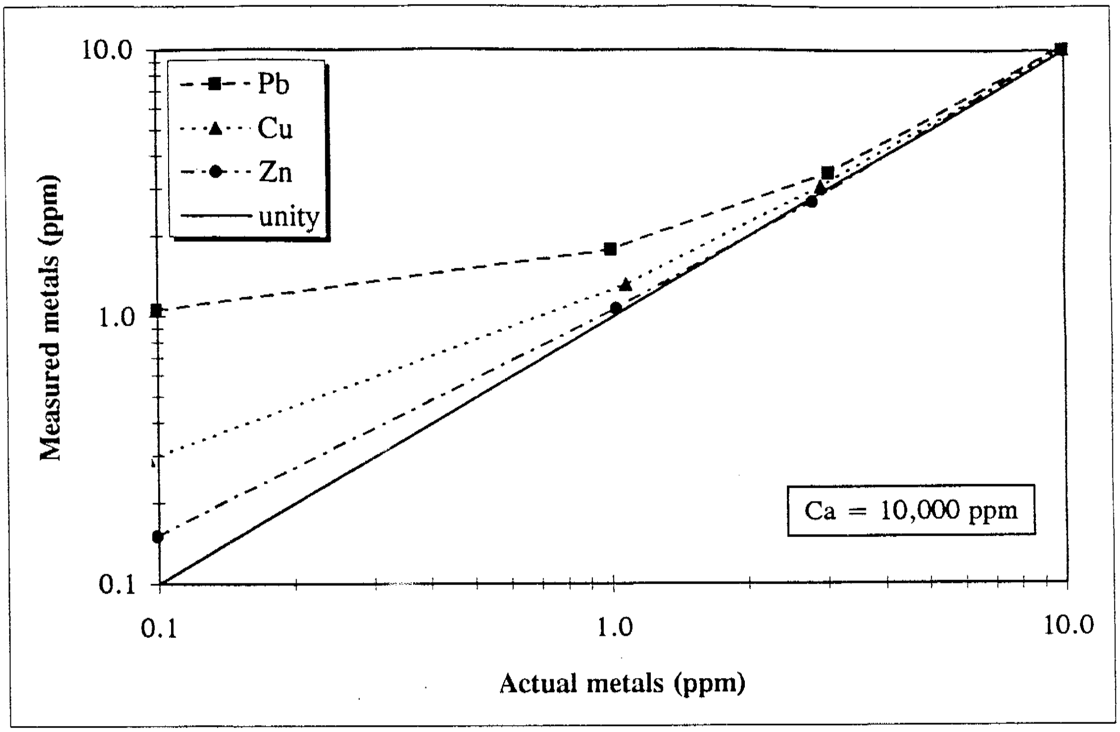

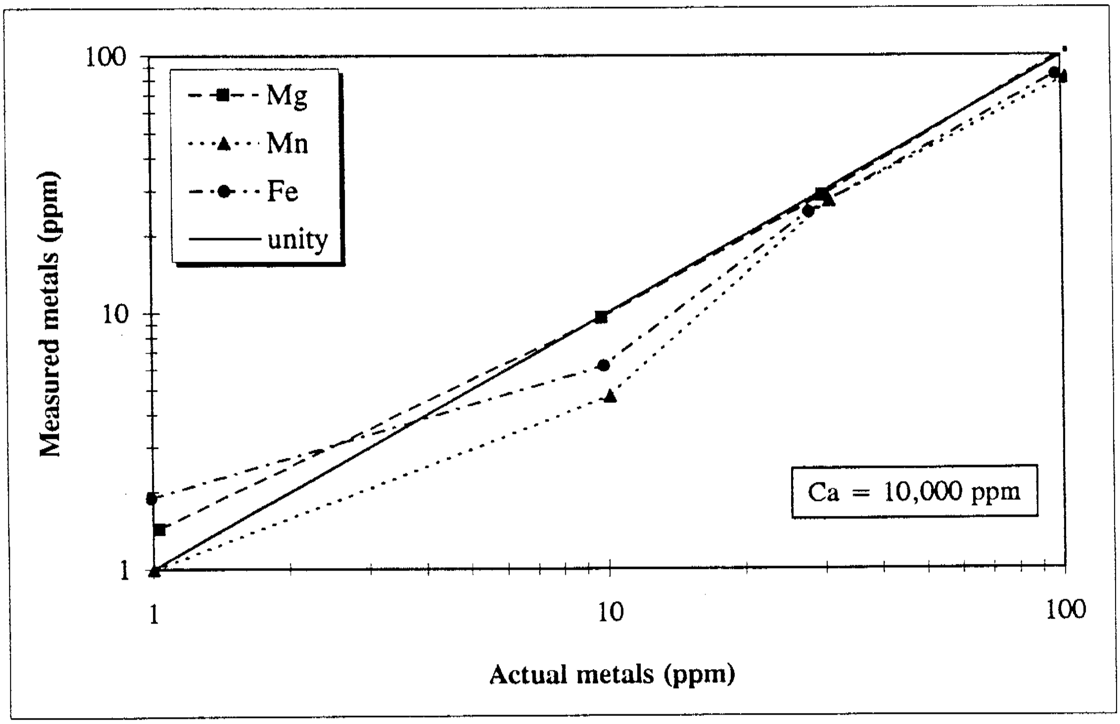

Fig. 2. Difference between measured and actual concentration for metals in dissolved calcite samples, due to a constant high calcium concentration. Analytic error equal to width of the symbols.

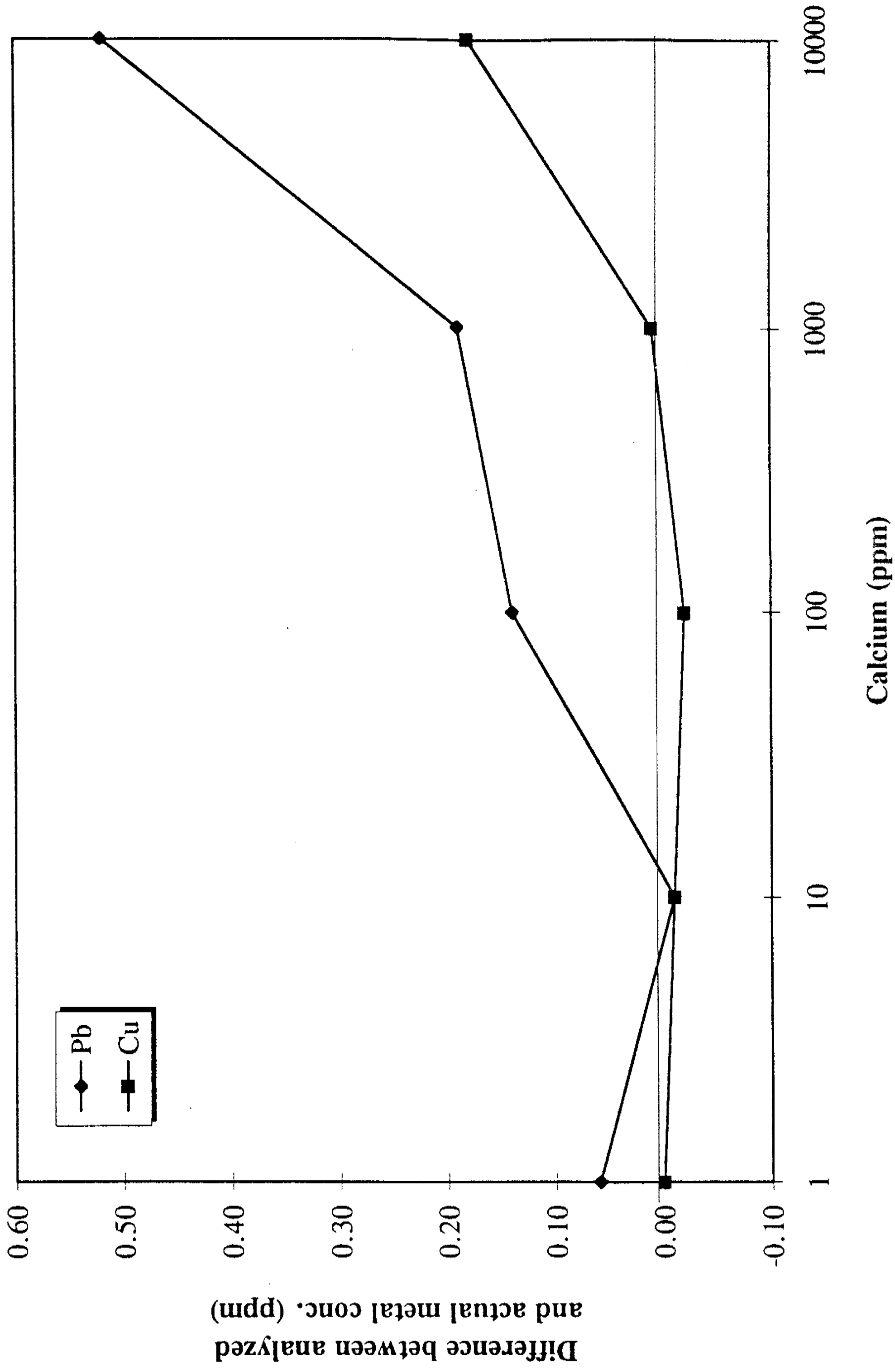

Fig. 3. Difference between measured and actual concentration for metals in dissolved calcite samples at varying calcium concentrations. Analytic error equal to width of the symbols.

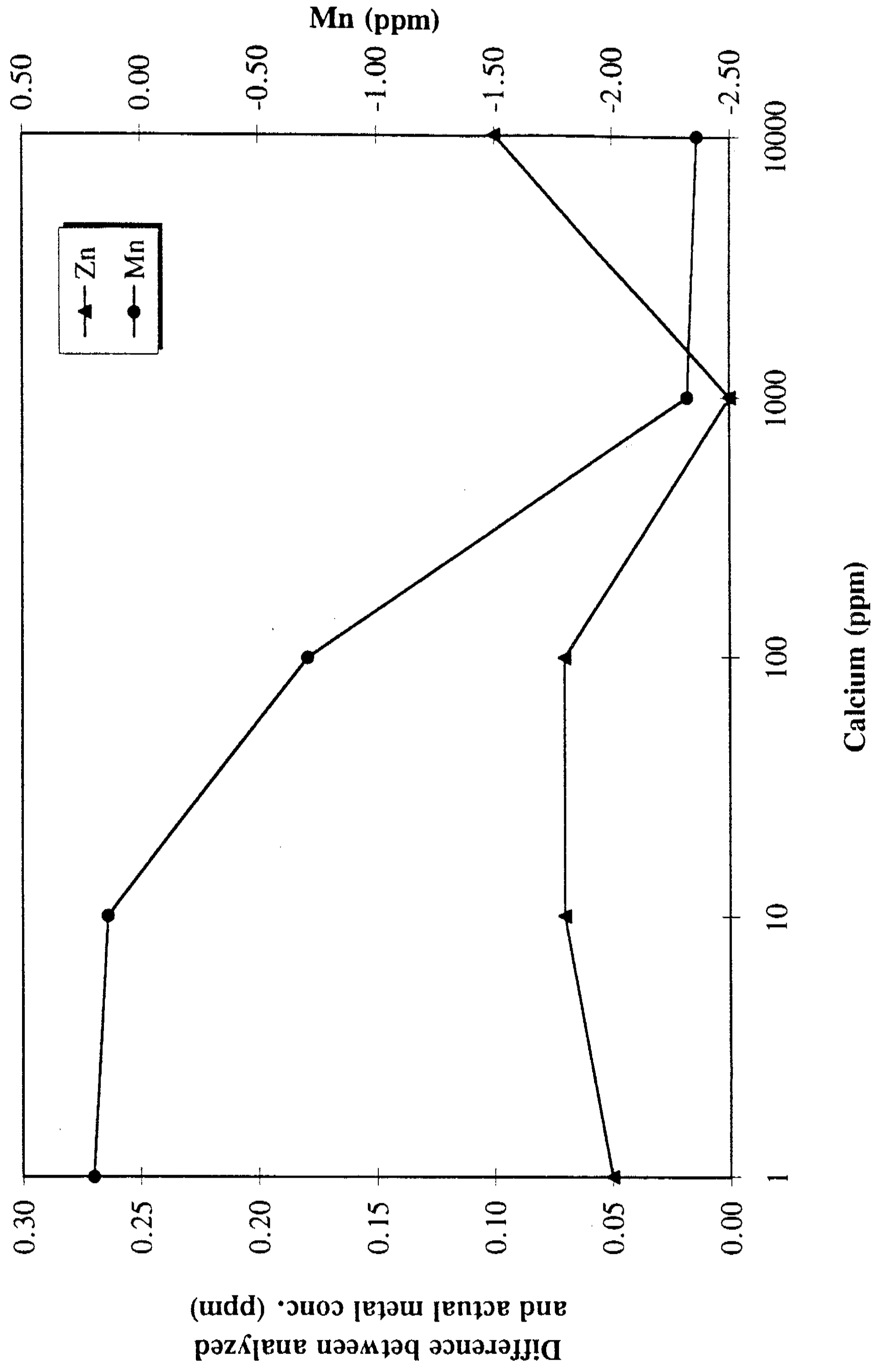

Fig. 4. Difference between measured and actual concentration for metals in dissolved calcite samples at varying calcium concentrations. Analytic error equal to width of the symbols.

Ion exchange chromatography

Ion exchange chromatography is a means of separating aqueous species of various sizes and charges. A resin material, Diphonix® (Eichrom, Inc.), was used to separate divalent metal cations from calcium ions. Diphonix consists of diphosphonic sites that absorb cations from solutions under acidic conditions, and this resin can be completely regenerated. Diphonix also separates ions based on their net charge (Fig. 5). It absorbs Cu^{2+}, Zn^{2+}, Pb^{2+}, and Mn^{2+}, and to a lesser extent Fe^{2+}; all unabsorbed ions pass through in the effluent solution (Kingston, et al., 1978).

The Diphonix resin used for these experiments was between 50 and 100 mesh and stored in distilled, deionized water. The density of the resin was slightly greater than pure water. About 10 grams (wet) was placed in 100 ml, 1.5 cm inner-diameter burettes; the bottom of each burette was fitted with glass wool to keep the resin in place. The volume of 10 g of resin was 12-14 cm^3 and its height in the burette was 8 cm.

Diphonix was first converted to the calcium saturated state; in this form, Diphonix absorbs divalent cations with ionic radii larger than calcium, while rejecting calcium ions. The resin was saturated with Ca^{2+} by passing 100 bed volumes of 0.02 M calcium hydroxide solution through it. As calcium passed through the resin, the pH of the effluent liquid was monitored to determine when the conversion was complete. Since calcium ions replace H^+ ions in the resin, once the pH of the effluent rose above 9, the resin was assumed to be converted to the calcium form. Distilled, deionized water was used to flush the resin of any extraneous calcium. During the water flush step, the pH of the effluent was monitored; the resin was assumed to be rinsed once the pH dropped below 9.

Ion exchange resin calibration

Before the ion exchange resin was used on the calcite samples, the resin was tested to gauge its ability to separate metal cations from calcium and to determine the best procedures for cation separation. Four burettes containing Diphonix resin were prepared. Four multi-element standards containing copper, lead, and calcium were made with varying metal and calcium concentrations (Table 9). The pH of the standards was adjusted to 4 using analytical grade ammonium hydroxide (NH_4OH; Mallinckrodt). Measured aliquots of 85 to 110 grams of standard solution were poured into each burette (this is similar to the amount of solution

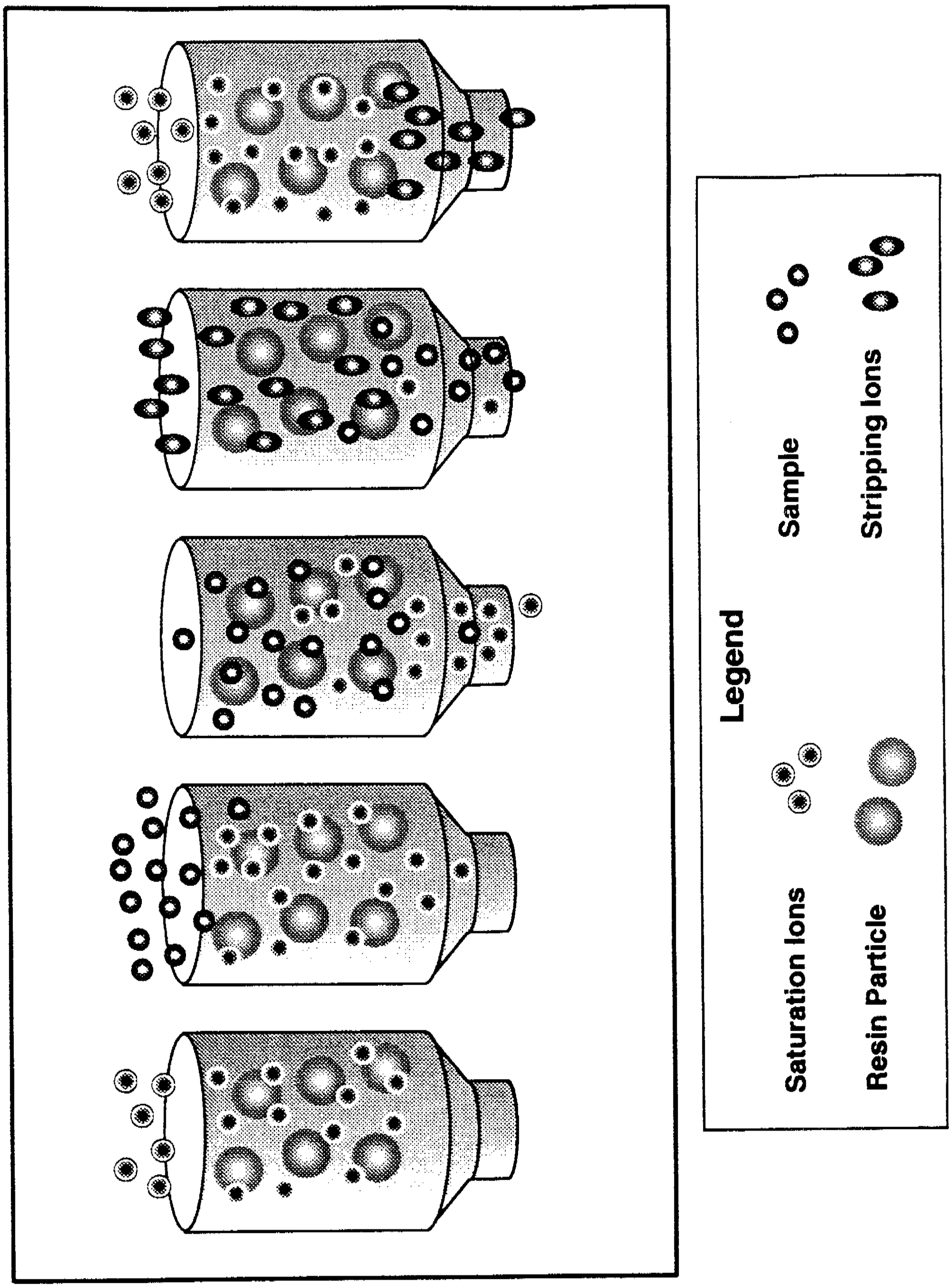

Fig. 5. Illustration of ion exchange chromatography. (A) Resin is saturated with solution containing cations to be separated (i.e., Ca). (B and C) Sample application and adsorption. In (D), ions from stripping solution (HCl) displace sample ions. Regeneration (E) - saturation ions displace stripping ions and resin is ready for next sample (modified from Bio-Rad Labs., Inc., 1995).

Table 9. Compositions of the four solutions used for resin test no. 1.

Sample	Pb (ppm)	Cu	Zn	Mn	Ca
A	0.095	0.106	0.098	0.929	9520
B	0.943	0.923	1.11	9.29	9560
C	2.72	3.07	2.59	26.48	9240
D	9.51	8.87	8.90	87.44	9010

generated by dissolving about 5 g of calcite). Then an aliquot of 20 grams of distilled, deionized water was used to displace the samples from the resin bed, followed by 15 grams of 0.05 M HCl to flush calcium from the resin. A final addition of 150 grams of 3.0 M HCl was used to liberate the metals from the resin. The first 105 ml of effluent was collected in aliquots of 45, 35, and 25 ml; the remaining 150 ml as 5 to 10 ml aliquots.

Analyses indicated separation of calcium and the metal cations (Fig. 6). This procedure, however, was not complete, as the recovery of the metal cations loaded on the column ranged from 29 to 97% (Table 10). Since such a large amount of sample was used, there was doubt as to whether the resin absorbed all the metals present. The volume of each test sample was at least 85 ml, which is about 6 times that of each resin bed. Hydrogen ions in the large test samples may have liberated metal cations first absorbed on the resin. Two new standards were prepared for the second calibration test (Table 11), as was done for the previous test, at a pH = 4. Between 13 and 15 grams were poured into each burette, followed by 20 ml of 0.05 HCl (adjusted to a pH of 4) to displace the standard. Then 120 ml of 3.0 M HCl was placed into each burette to remove the metals. The effluent was collected as 10 ml aliquots.

The results clearly indicate the separation between calcium and the metal cations, as well as the breakout point for the metal cations (Fig. 7). The first 50 ml of effluent contained $\geq$ 85% of calcium collected during the test. After 60 ml of effluent, the amount of calcium decreased sharply, allowing the metals in solution to be detected more accurately. The total amount of Pb and Cu collected was less than the amount placed in the burettes (Table 12).

The third resin test followed a procedure similar to the second test, with a few changes. Four standards were prepared of varying chemistry (Table 13) with the pH adjusted to 3.3 using 10-30 ml NH_4OH. Between 12 and 15 grams of solution were poured into the burettes, followed by 20 ml of 0.05 HCl. Finally, 100 ml 3.0 M HCl was added to remove the metals from the resin.

The results verify what was learned from test 2. The first 60 ml of effluent contained the highest calcium concentration, the next 45 ml had most of the metals, and the remaining 35 ml had a lower amount of metals, yet at concentrations above the detection limit (Table 14). As in the second test, the third resin test showed that after the first 60 ml of effluent passed through the resin, the calcium concentration decreased significantly (Fig. 8.a, b). Also, the recovery percentage of the cations was calculated as before (Table 15). A larger amount of calcium was measured in the effluent than what was added to the columns for reasons described below.

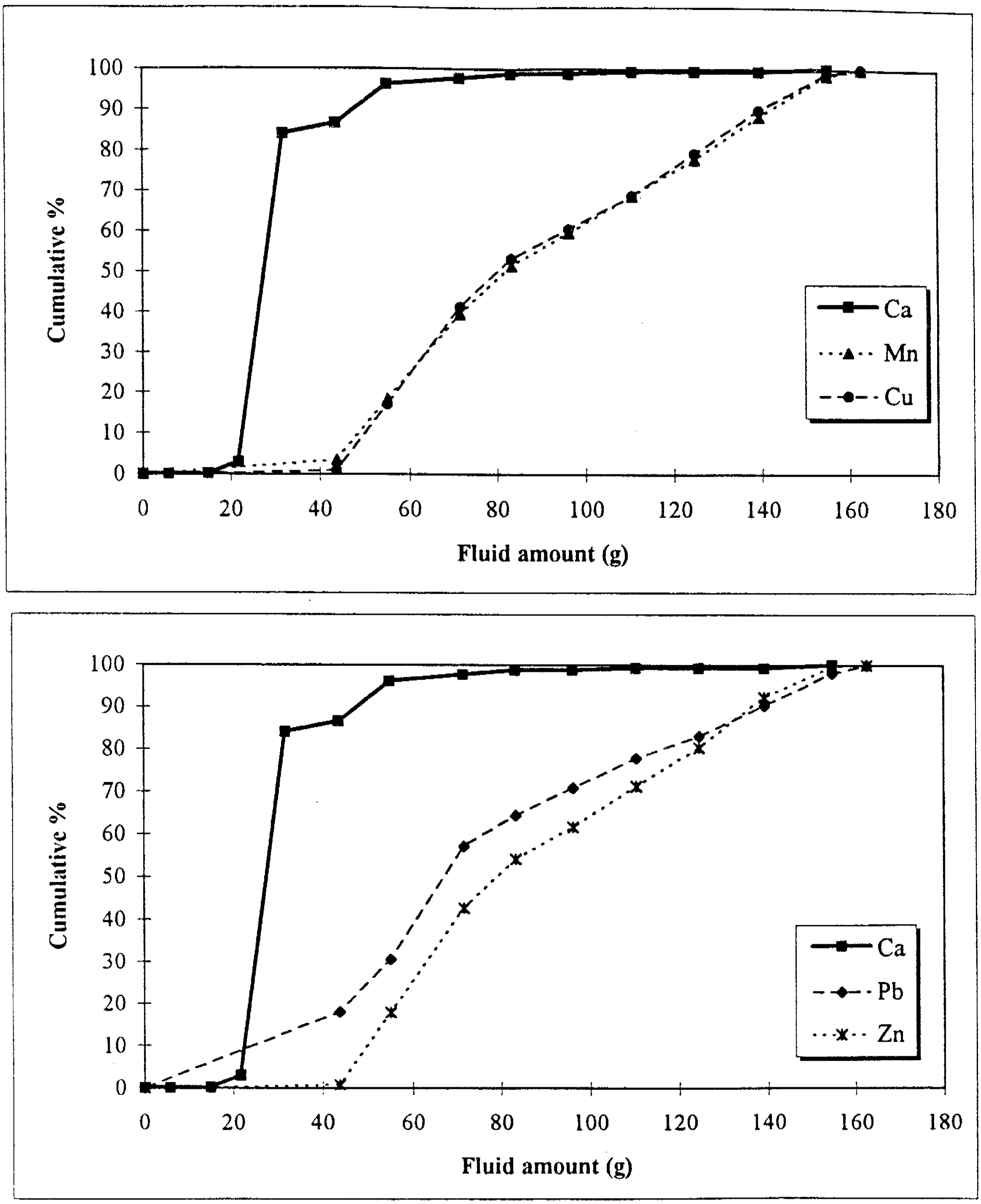

Fig. 6. Cumulative frequency diagram for calcium and metals analysis of dissolved calcite samples, resin test no. 1. Analytic error equal to width of the symbols.

Table 10. Recovery percentage for metals, resin test no. 1.

Sample	Pb (%)	Cu	Zn	Mn
A	81.5	75.7	n.d.	96.5
B	41.4	45.2	59.4	42.9
C	67.1	87.5	56.6	34.3
D	10.2	9.58	9.61	94.4

n.d.: No data

Table 11. Compositions of the two solutions used for resin test no. 2.

Sample	samp. wt. (g)	Pb (ppm)	Cu	Ca
A	13.15	0.10	0.10	9795
B	14.34	0.25	0.26	26113

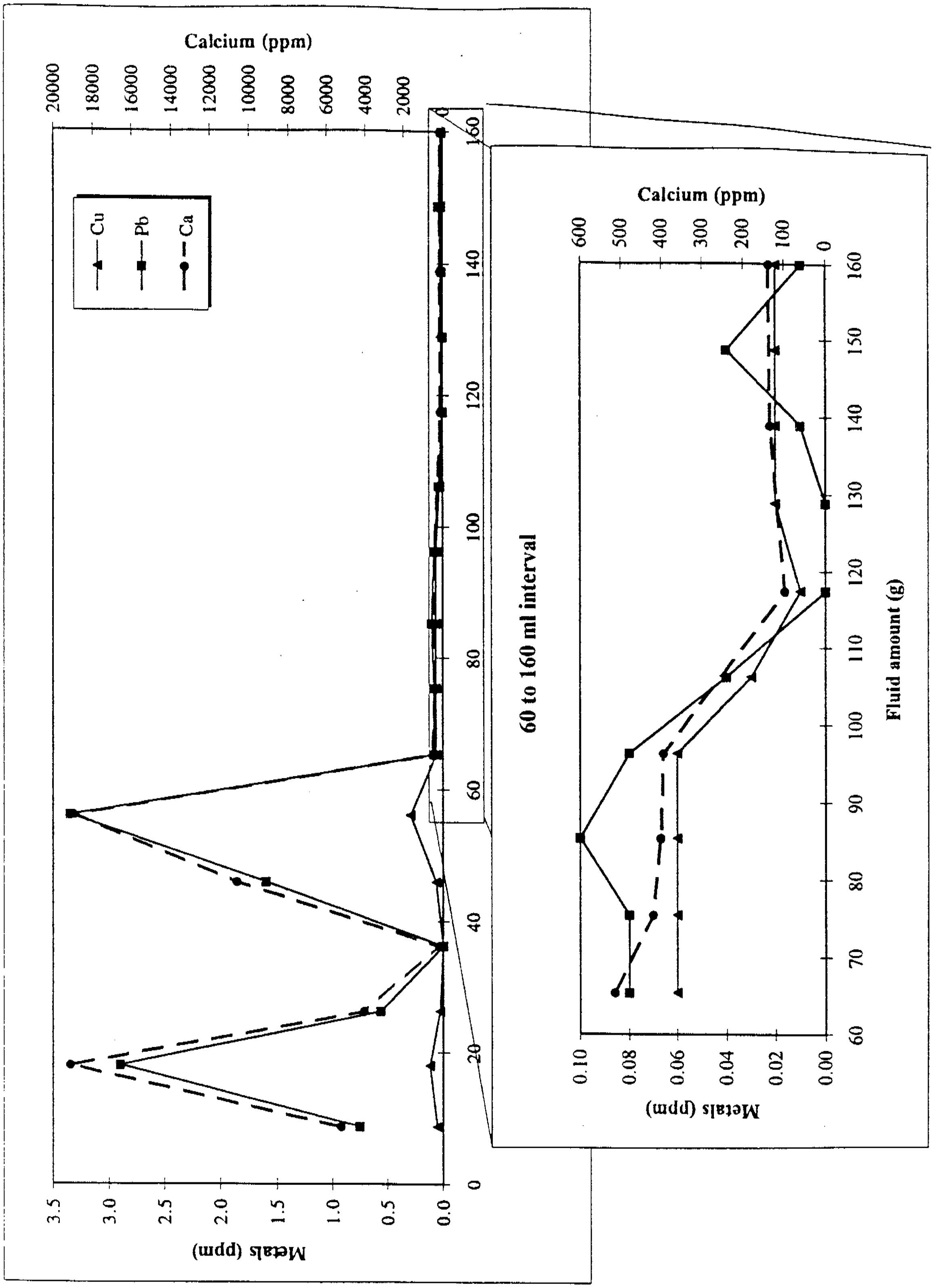

Fig. 7. Analytical results of Cu, Pb, and Ca from resin calibration test no. 2. Analytic error equal to width of the symbols.

Table 12. Recovery percentage for metals, resin test no. 2.

Sample	Pb (%)	Cu
A	33.7	81.3
B	12.5	n.d.

n.d.: no data

Table 13. Compositions of the four solutions used for resin test no. 3.

Sample	Pb (ppm)	Cu	Zn	Mn	Ca
A	0.08	0.08	0.08	0.86	8543
B	0.95	0.97	0.93	10.41	10159
C	10.64	9.37	10.88	99.7	10214
D	270.1	91.3	271.1	144.3	10169

Table 14. Concentrations of metals in aliquots, resin test no.3, sample A.

concentration	Pb (ppm)	Cu	Zn	Mn	Ca
aliquot 1	0.31	0.14	0.26	0.24	480
aliquot 2	0.25	0.10	0.13	0.13	398
detection limit	0.15	0.05	0.05	0.10	0.50

Table 15. Recovery percentage for cations in resin test no.3.

Standard	Pb (Rec. %)	Cu	Zn	Mn	Ca
A	n.d.	n.d.	n.d.	n.d.	437
B	89.6	64.1	n.d.	61.7	398
C	44.8	38.3	79.2	37.1	337
D	50.6	52.5	52.8	43.6	376

n.d.: no data

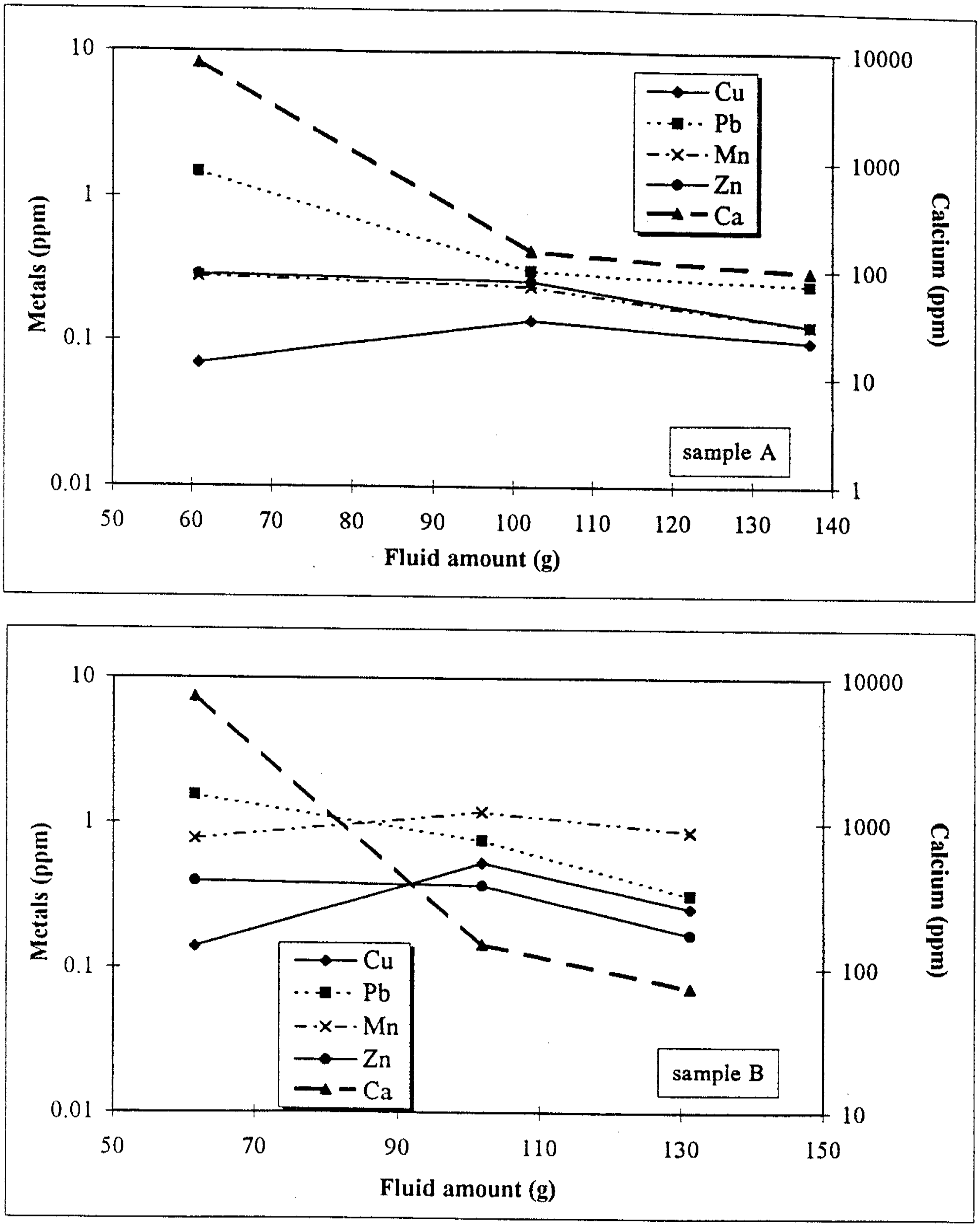

Fig. 8a. Analytical results of Cu, Pb, Zn, Mn, and Ca from resin calibration test no. 3, samples A and B. Analytic error equal to width of the symbols.

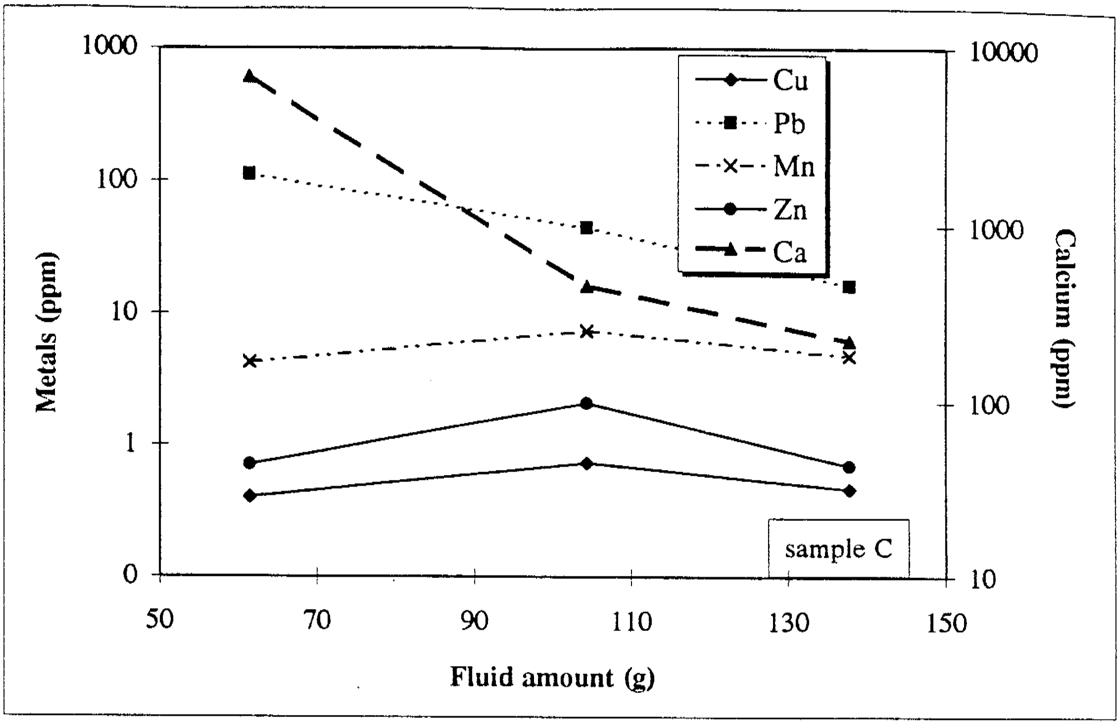

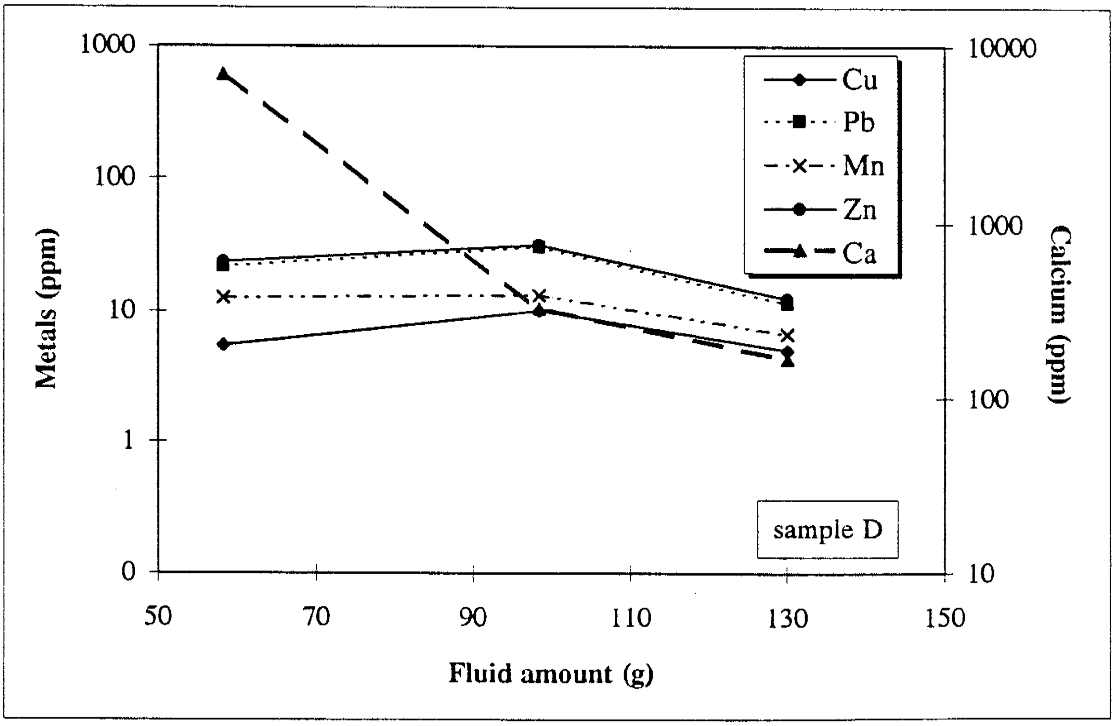

Fig. 8b. Analytical results of Cu, Pb, Zn, Mn, and Ca from resin calibration test no. 3, samples C and D. Analytic error equal to width of the symbols.

These calibration tests outlined the ability of Diphonix to separate calcium from metal cations. Furthermore, they provided data showing the separation point for calcium and the metal cations and the point at which calcium concentration decreased in the effluent (Figs. 6 and 7). Figure 5 illustrates the cumulative collection of the metals in resin test 1. Eighty-five percent of the calcium was collected in the first 30 ml of effluent. In the first 65 ml, only 20% of the metals were detected. This was an apparent detection, since it was difficult to quantify the amount of metals in solutions of high calcium concentration. It was assumed that a small portion of the metals was present in the initial fraction of the effluent, causing the recovery percentage for the metal cations to be less than 100. In resin test 2, the majority of the calcium was collected in the first 55 ml of effluent (Fig. 7). Since standards were used to calibrate the resin, we determined the recovery percentage for calcium and the metals (Table 16). In all cases, a larger amount of calcium was collected than added. Since the resin was saturated with $Ca(OH)_2$ before use (as described above), extra calcium was flushed out when the slightly acidic standards were loaded. This may explain the high concentration of calcium in the first 20 ml of effluent. Furthermore, at low metal concentrations, analytical detection is subject to calcium interference (Fig. 2). Although the amount of calcium in aliquots 1 and 2 was less than 500 ppm, standard A in resin test 3 may have been affected slightly by calcium interference (Table 15).

Ion exchange chromatography for samples

Considering the above ion exchange resin tests, the following procedure was followed for the analysis of calcite for Cu, Pb, Zn, and Mn. The pH of the dissolved calcite was adjusted to 3.3 and the procedure used for the third resin test were followed. After completing the ion exchange chromatography, dilutions of all aliquots were made for calcium analysis, and the second and third aliquots were evaporated (when necessary) for metal analysis. Between each sample run, the ion exchange resin was first flushed with distilled, deionized water and then converted to the calcium form in the manner described above. The data produced from AA analysis were standardized to the initial amount of calcite dissolved:

$$\%M_{cal} = [(C_1 w_1 + C_2 w_2)/w_{samp}](w_{tot} w_{cal}) \times 100 \qquad (30),$$

where $\%M_{cal}$ is the percent of Cu, Pb, Zn, and Mn in calcite. C_1 and C_2 are the concentrations (parts per million) of each cation in aliquots 1 and 2. The mass of aliquots 1 and

2 are listed as w_1 and w_2 (in grams). The mass of the liquid sample added to the ion exchange resin is w_{samp}, the total amount of solution resulting from acid digestion of the calcite sample is w_{tot}, and the amount of calcite dissolved is w_{cal} (grams). These values were normalized against calcite standards to account for background anomalies encountered due to ion exchange chromatography procedures.

Dissolved calcite samples were measured directly for Mg and Fe using AA. Ion exchange chromatography was not used to separate these cations from Ca because the resin used (Diphonix) does not preferentially adsorb Mg or Fe (II) over Ca. Also, the concentrations of Mg and Fe were high enough to avoid problems caused by Ca matrix interference patterns (Fig. 2). The concentration of Mg or Fe in calcite is determined by equation 2:

$$\%\mathbf{M}_{cal} = \mathbf{C}_A(\mathbf{w}_{tot}/\mathbf{w}_{cal}) \times \mathbf{100} \qquad \mathbf{(31).}$$

The symbol C_A is the concentration of Mg or Fe collected directly using AA. The other symbols are the same as those in equation 1.

RESULTS

Chemistry data

Fifteen calcite samples were measured for Cu, Pb, Zn, Mg, Fe, and Mn using atomic absorption spectrophotometry, as well as water samples from Coso 8, Coso 20, and DV; other water data was obtained from previous analyses (Table 16, Fig. 9). The analytical results for calcite data are listed in Appendix B. All measurements less than the analytical detection limit for each element (Table 7) were disregarded. To account for matrix scattering effects caused by dissolved solids in the samples, correction values were subtracted from the AA data for Cu, Pb, Zn, and Mn, depending on the concentration of calcium in the samples (Table 17). These correction values are equivalent to the analytical error caused by calcium interference. Furthermore, element readings less than 1.5 times the adjustment factor were also considered to be suspect. For example, the adjustment factor is 0.14 ppm for lead in liquid samples with 100 ppm calcium; consequently, any reading less than 0.21 ppm lead was disregarded. This limit was chosen due to the amount of analytical variation (expressed as relative standard deviation) during most sample measurements.

The corrected data for the metal concentrations in the liquid samples were then employed to compute the initial calcite chemistry. To calculate Cu, Pb, Zn, and Mn concentrations in calcite, equation 30 listed above was used and equation 31 was used to calculate Mg and Fe concentrations.

Using the equations for solid solution chemistry listed previously, the composition of the parent water was calculated from the composition of the analyzed calcite. Similarly, theoretical calcite compositions were calculated from analyzed water data (Table 18, 19; Fig.10, 11).

Obviously, the analyzed compositions of calcite and water do not correspond exactly to the calculated counterparts (Table 18, 19; Fig. 10, 11); reasons for this are discussed below. However, for some of the samples (TBG, BR, NT), there is a general correlation relating the calculated and actual compositions (Fig. 12, 13).

ppm	Cu		Pb		Zn		Mg		Fe	
	water	calcite	water	calcite	water	calcite	water	calcite	water	calcite
DV	0.009	0.676	0.078	0.976	0.015	N.D.	0.123	74.87	0.086	458.6
COSO 8-A	0.027	0.792	0.115	1.868	0.007	5.190	0.076	3861.5	0.096	141.9
COSO 8-B	0.027	N.D.	0.115	N.D.	0.007	4.867	0.076	3632.7	0.096	141.7
COSO 20-A	0.065	1.534	0.215	16.57	0.020	6.925	0.038	3009.6	0.318	785.5
COSO 20-B	0.065	N.D.	0.215	N.D.	0.020	3.920	0.038	2590.6	0.318	627.7
*NT-A	0.010	1.474	0.010	0.712	0.010	N.D.	2.300	28.91	0.290	406.7
*NT-B	0.010	N.D.	0.010	N.D.	0.010	N.D.	2.300	64.64	0.290	314.4
*NT-C	0.010	N.D.	0.010	N.D.	0.010	5.372	2.300	37.09	0.290	315.4
BR11-A	0.001	0.632	0.002	2.291	0.009	4.765	0.590	3544.1	0.230	627.3
BR11-B	0.001	N.D.	0.002	N.D.	0.009	N.D.	0.590	3575.9	0.230	659.6
TBG	171.0	0.176	N.D.	0.176	1240.0	2.532	19200.0	71.84	N.D.	176.1
SSDP-A	6.000	0.627	95.00	0.487	506.0	N.D.	36.00	463.7	1550	1801.1
SSDP-B	6.000	N.D.	95.00	N.D.	506.0	0.842	36.00	434.7	1550	1692.2
SSDP-D	6.000	N.D.	95.00	N.D.	506.0	N.D.	36.00	N.D.	1550	N.D.
VC2B	N.D.	0.881	N.D.	1.760	N.D.	5.249	0.760	1331.9	15.10	2732.1

*water values for Cu, Pb, Zn estimated N.D.:Not detected

Table 16. Analyzed composition of water vs. analyzed composition of calcite.

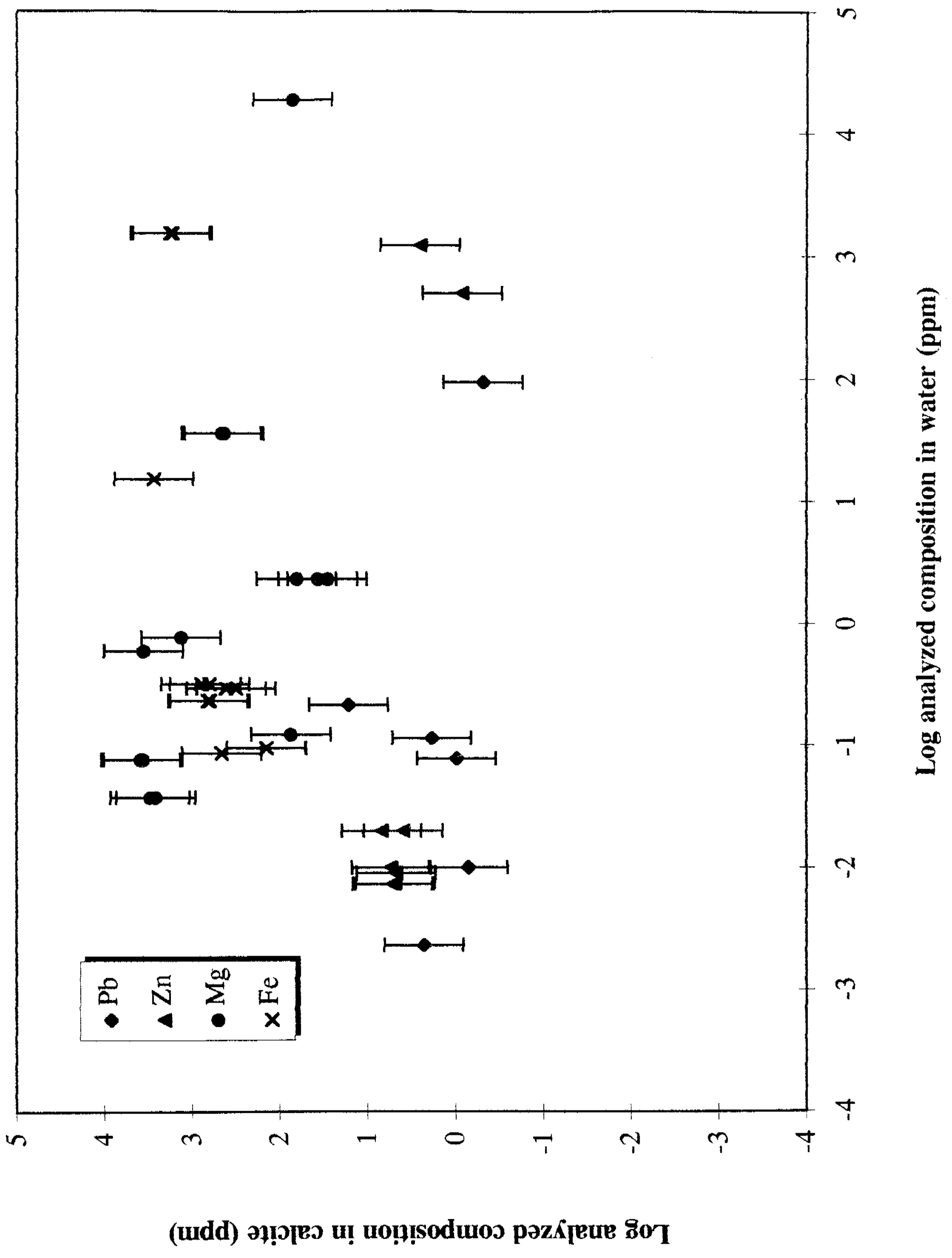

Fig. 9. Analytical chemistry results: calcite sample analyses versus parent fluid analyses. Y-axis error is equal to 451%; X-axis error is equivalent to width of the symbols (30%).

Table 17. Analytical measurement error for dissolved calcite samples as a function of calcium concentration in solution.

		Pb	Cu	Zn	Mn
Ca concentration		2.0 ppm	0.5	0.5	5.0
ppm	0	0.08	-0.01[1]	0.06	0.10
	1	0.06	0.00	0.05	0.20
	10	-0.01	-0.01	0.07	0.14
	100	0.14	-0.02	0.07	-0.71
	1000	0.19	0.01	0.00	-2.32
	10000	0.52	0.18	0.10	-2.36

[1] a negative value indicates that the measured value was less than the actual concentration in solution.

ppm	Cu		Pb		Zn		Mg		Fe	
	analysis	calculated	analysis	calculated	analysis	calculated	analysis	calculated	analysis	calculated
DV	0.676	0.534	0.976	118.4	N.D.	11.25	74.87	767.5	458.6	3099.1
COSO 8-A	0.792	0.019	1.868	1.323	5.19	0.044	3861.5	25.52	141.9	34.56
COSO 8-B	N.D.	0.019	N.D.	1.323	4.87	0.044	3632.7	25.52	141.7	34.56
COSO 20-A	1.534	0.016	16.57	0.998	6.93	0.044	3009.6	5.074	785.5	39.52
COSO 20-B	N.D.	0.016	N.D.	0.998	3.92	0.044	2590.6	5.074	627.7	39.52
*NT-A	1.474	0.047	0.712	0.448	N.D.	0.227	28.91	384.8	406.7	667.4
*NT-B	N.D.	0.047	N.D.	0.448	N.D.	0.227	64.64	384.8	314.4	667.4
*NT-C	N.D.	0.047	N.D.	0.448	5.37	0.227	37.09	384.8	315.4	667.4
BR11-A	0.632	0.032	2.291	1.402	4.77	2.906	3544.1	1888.0	627.3	4414.0
BR11-B	N.D.	0.032	N.D.	1.402	N.D.	2.906	3575.9	1888.0	659.6	4414.0
TBG	0.176	0.105	0.176	N.D.	2.53	0.461	71.84	210.2	176.1	N.D.
SSDP-A	0.627	0.062	0.487	0.672	N.D.	2.095	463.7	4.858	1801.1	1752.2
SSDP-B	N.D.	0.062	N.D.	0.672	0.84	2.095	434.7	4.858	1692.2	1752.2
SSDP-D	N.D.	0.062	N.D.	0.672	N.D.	2.095	N.D.	4.858	N.D.	1752.2
VC2B	0.881	N.D.	1.760	N.D.	5.25	N.D.	1331.9	37.63	2732.1	2231.9

*calculated values for Cu, Pb, Zn estimated N.D.:Not detected

Table 18. Results for calcite samples: calculated compositions vs. analyzed compositions.

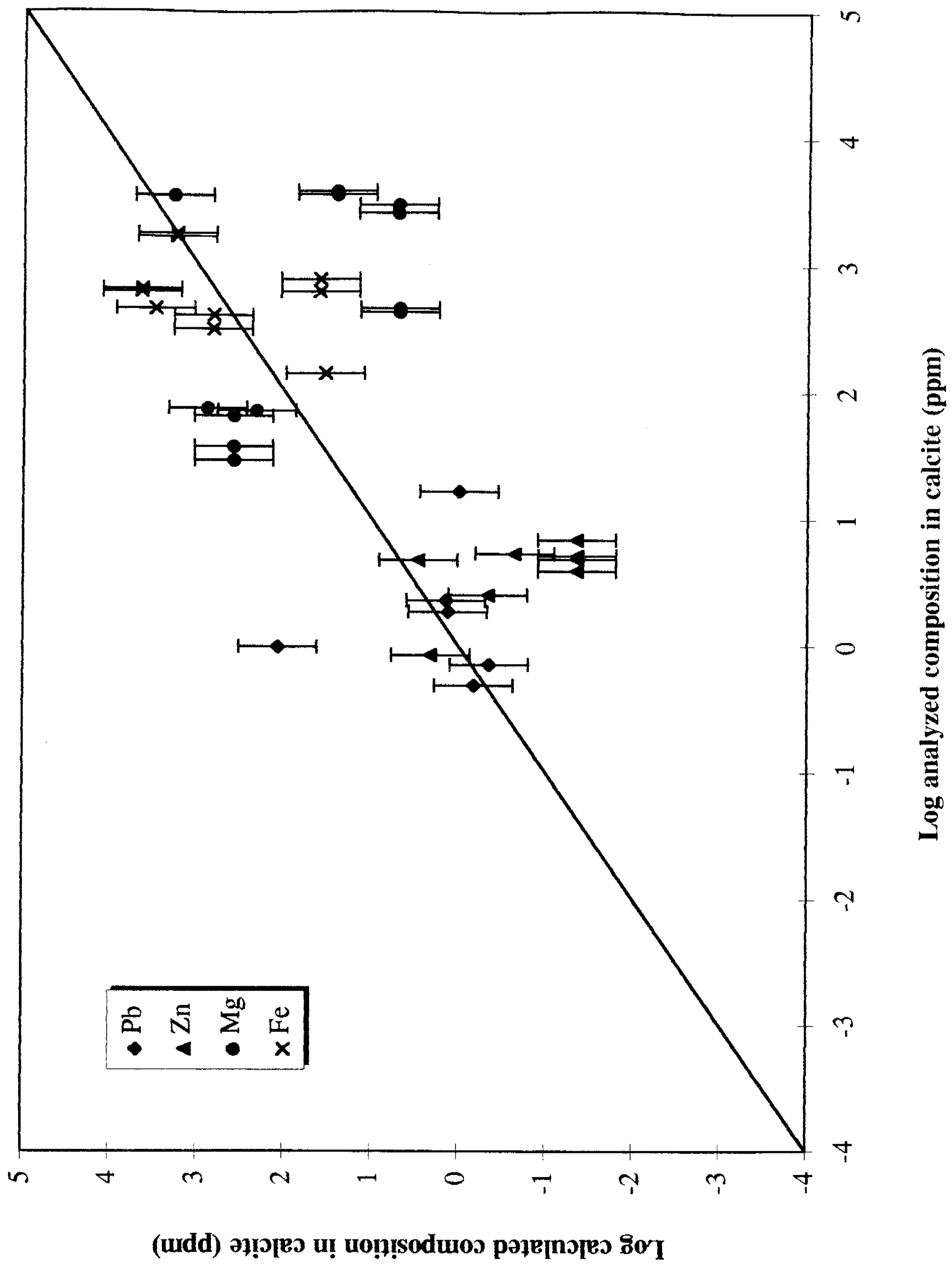

Fig. 10. Calculated vs. analyzed chemistry of calcite samples. Y-axis error is equal 451%; X-axis error is equivalent to the width of the symbols (30%).

ppm	Cu		Pb		Zn		Mg		Fe	
	analysis	calculated	analysis	calculated	analysis	calculated	analysis	calculated	analysis	calculated
DV	0.009	0.012	0.078	0.001	0.015	N.D.	0.123	0.012	0.086	0.013
COSO 8-A	0.027	1.104	0.115	0.162	0.007	0.866	0.076	11.46	0.096	0.392
COSO 8-B	0.027	N.D.	0.115	N.D.	0.007	0.812	0.076	10.78	0.096	0.392
COSO 20-A	0.065	6.242	0.215	3.574	0.020	3.133	0.038	22.20	0.318	6.317
COSO 20-B	0.065	N.D.	0.215	N.D.	0.020	1.773	0.038	19.11	0.318	5.049
*NT-A	0.010	0.314	0.010	0.016	0.010	N.D.	2.300	0.175	0.290	0.177
*NT-B	0.010	N.D.	0.010	N.D.	0.010	N.D.	2.300	0.391	0.290	0.137
*NT-C	0.010	N.D.	0.010	N.D.	0.010	0.236	2.300	0.224	0.290	0.137
BR11-A	0.001	0.020	0.002	0.004	0.009	0.015	0.590	1.106	0.230	0.033
BR11-B	0.001	N.D.	0.002	N.D.	0.009	N.D.	0.590	1.116	0.230	0.034
TBG	171.0	285.3	N.D.	284.2	1240.0	6816.8	19200.0	6563.0	N.D.	1821.2
SSDP-A	6.000	110.0	95.00	195.0	506.0	N.D.	36.00	9956.4	1550	1593.2
SSDP-B	6.000	N.D.	95.00	N.D.	506.0	587.5	36.00	9333.7	1550	1496.9
SSDP-D	6.000	N.D.	95.00	N.D.	506.0	N.D.	36.00	N.D.	1550	N.D.
VC2B	N.D.	2.683	N.D.	0.856	N.D.	3.794	0.760	26.87	15.10	18.49

*analyzed values for Cu, Pb, Zn estimated N.D.:Not detected

Table 19. Results for parent fluid samples: calculated compositions vs. analyzed compostions.

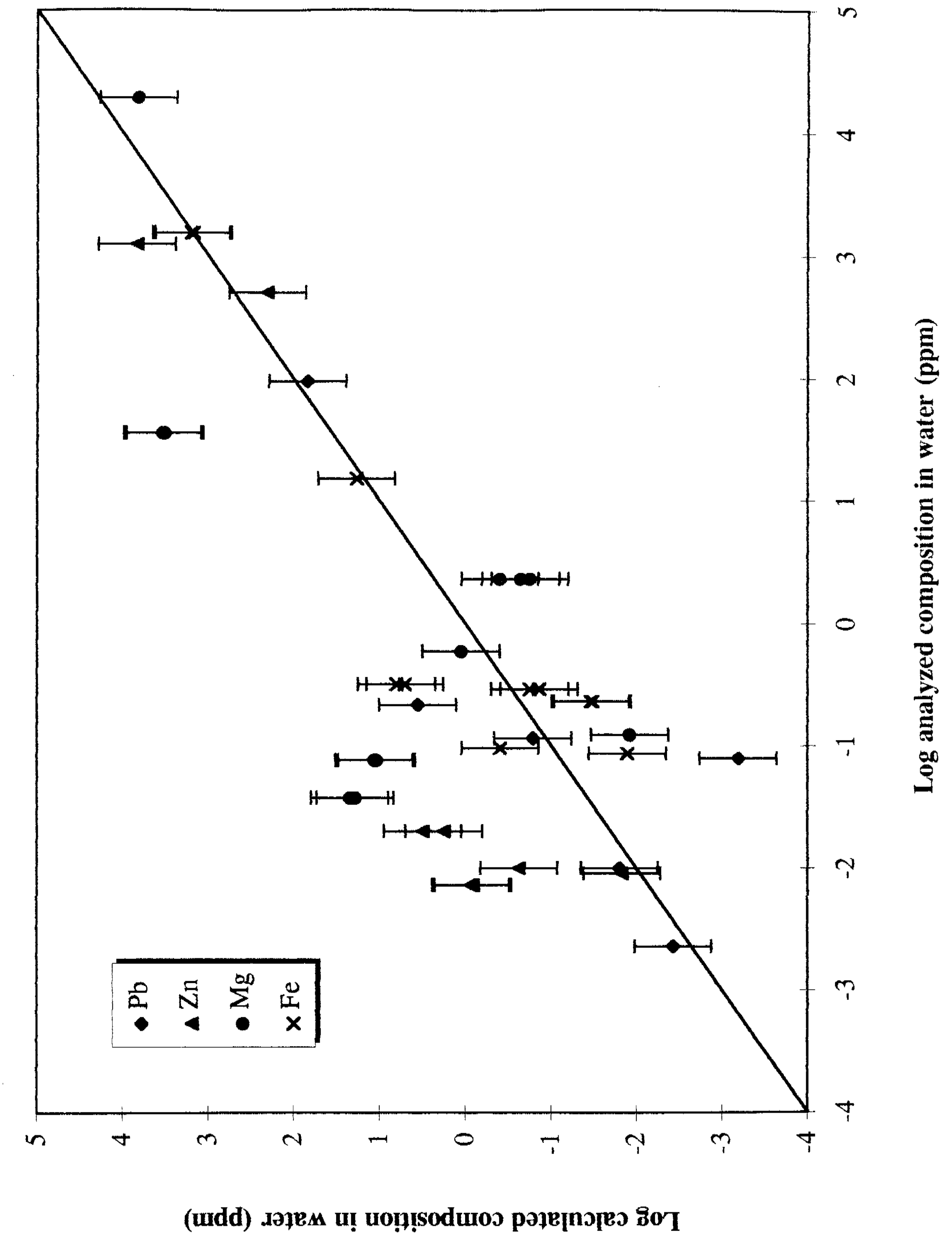

Fig. 11. Calculated vs. analyzed chemistry of parent fluid. Y-axis error is equal to 451%; X-axis error is equivalent to the width of the symbols (30%).

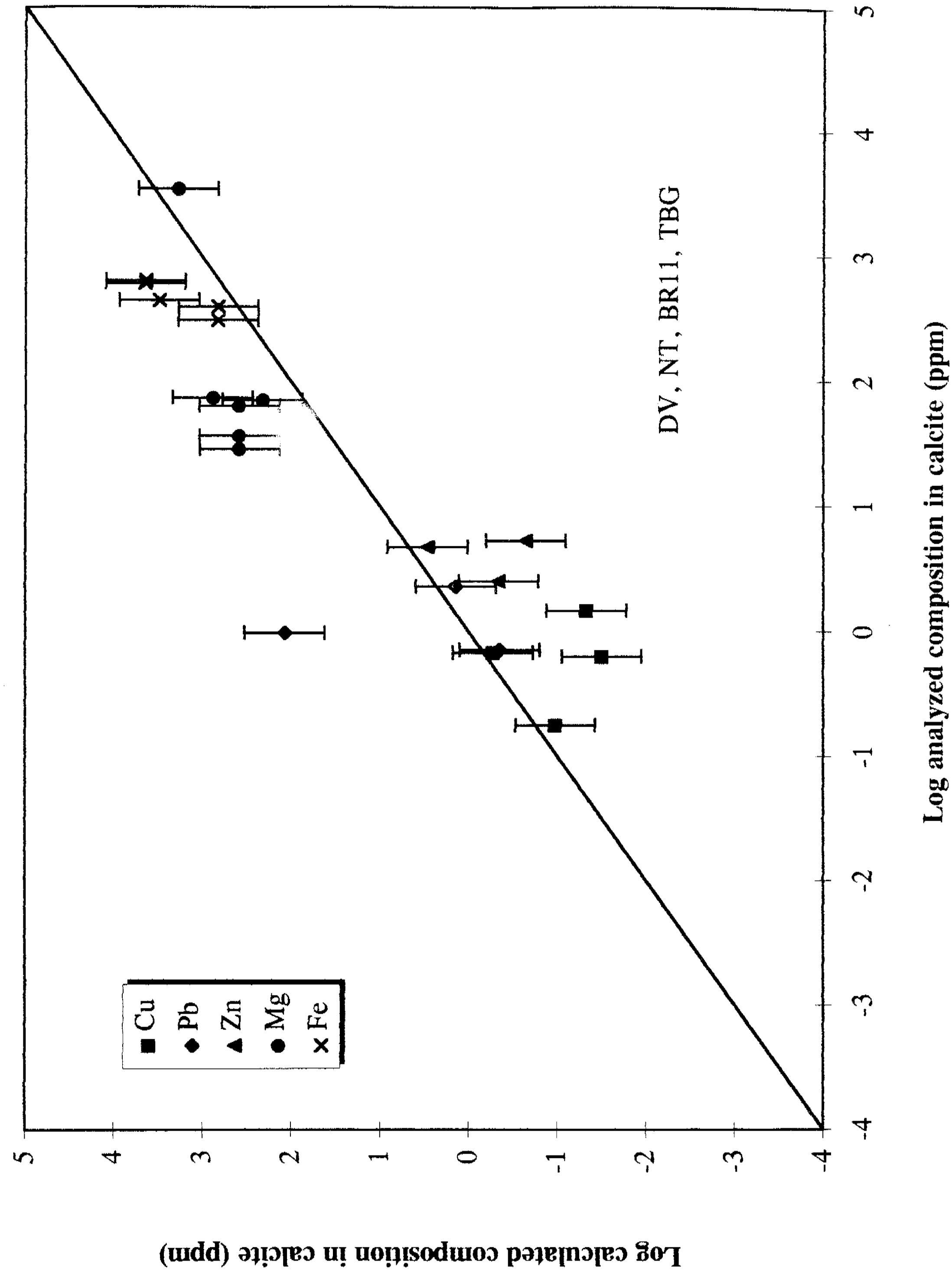

Fig. 12. Calculated vs. analyzed calcite chemistry for selected samples. Y-axis error is equal to 451%; X-axis error is equivalent to width of the symbols (30%).

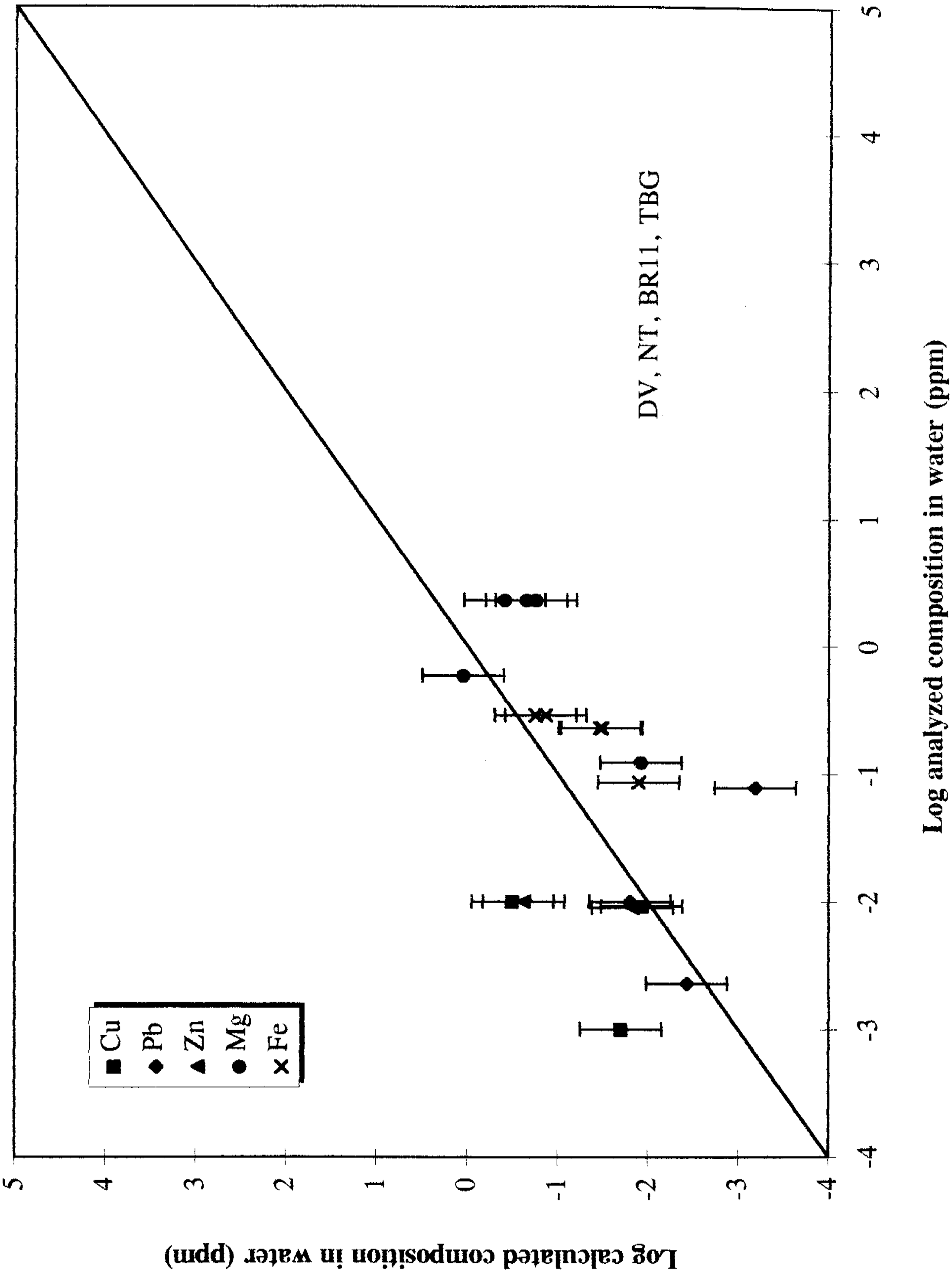

Fig. 13. Calculated vs. analyzed water chemistry, selected samples. Y-axis error is equal to 451%; X-axis error is equivalent to width of the symbols (30%).

Error measurement

Error determinations were calculated here considering possible sampling, measurement, and theoretical error. The following section defines the reasonable amounts of error that may explain the differences between the analytical measurements of divalent cations in calcite samples and the concentrations of such cations as calculated using solid solution chemistry relationships.

Calcite analysis error

The analytical error for cation measurements was determined by calculating the error of AA measurements; this is expressed as standard and relative standard deviation. The sample set mean was calculated from five automatic spectrophotometer readings of each. The standard deviation was also calculated automatically during analysis and is listed in parts per million for each element. The relative standard deviations; that is, the percent difference between the standard deviation of a sample set and the mean value of the set, are up to 30% for the sample sets (Appendix B).

A separate source of doubt lies in the preparation of the calcite for analysis. All measured samples were hand picked to eliminate non-calcite phases from the dissolved calcite. Yet some of the samples were finely banded, notably COSO 8 and STB (COSO 20 had calcite rhombs growing on the outside surface of the bladed calcite, see Appendix A). It seems logical that this results from multiple deposition periods; i.e., waters of different chemistry depositing calcite of different composition. However, in a geothermal environment, calcite is usually deposited as scale in pipes quite rapidly and it is assumed that the composition of dilute geothermal water remains relatively constant over the depositional time period.

Also, the formic acid used to dissolve calcite samples contained 0.51 ppm Fe; this amount was subtracted from Fe analyses to correct for this contamination. The formic acid used to dissolve the calcite samples was analyzed for all cations in question periodically; except for Fe, there were negligible amounts of the cations detected (Appendix B). Furthermore, there was concern that a proportion of the cations would form ionic complexes with the formate ion. However, all liquid samples run through the ion exchange resin were acidified to a pH of 3.3, thereby eliminating the possibility of the formate ion acting as a complexing agent (Shock and Koretsky, 1995).

Water analysis error

The loss of calcite as scale could alter the chemistry of the water by incorporating metals into the solid during deposition. Water chemistry variations are assumed to be minimal because of the large amount of fluid flowing through geothermal systems, even for saline systems (McKibben and Williams, 1989). However, if the water assumed to be the parent fluid did not in fact deposit the particular calcite sample from the same system, the water and the calcite were not in equilibrium and therefore comparisons of analyzed and calculated compositions are groundless.

The total amount of analytical error is estimated to 30%, taken from the relative standard deviation readings collected during calcite analysis.

Estimated error for calculated values

Aside from analytical error, we examined the inaccuracy involved in the theoretical calculations of calcite and water chemistry. An estimation of the error for calcite solid solution chemistry is determined from the equations listed on pages 1-4; possible error is summarized as follows:

temperature measurements:	± 15°C,
activity coefficient estimations	± 5 - 18% (as determined by ION),
cumulative formation constants	± 142% (ionic complexation between cations and anions).

The addition of these errors gives a total possible theoretical error of 451% for any one calcite sample.

Certain simplifications in these calculations contribute to the total error. For example, chloride is assumed to be the main complexing ligand in the calculations used for this study; however, metals in solution also form ionic complexes with other anion species (e.g., the bisulfide, hydroxide, and carbonate ions). However, considering geothermal systems, Weissberg, et al. (1979) showed that less than 0.05% of the total lead measured in solution at Broadlands exists as the most stable bisulfide complex, $Pb(HS)_3^-$, at such conditions (270°C, near-neutral pH). The amount of H_2S measured in solution at Broadlands ranges from 34 to 102 ppm (Henley, et al., 1984; Weissberg, et al., 1979).

Therefore, HS^- complexation is assumed to be negligible. The Broadlands calcite measured in this study is assumed to have precipitated from water with 0.002 ppm $Pb_{(tot.)}$. The amount of H_2S in solution is 102 ppm; therefore, the maximum amount of Pb (at 270°C and pH = 6.1) existing as a bisulfide complex is 2.3×10^{-6} ppm, or 0.1% of the total lead in solution. It is inferred that for most geothermal systems, the main complexing agent is chloride, even for systems of very high salinity (McKibben and Williams, 1989). Similar conclusions are verified for zinc (Table 4).

DISCUSSION

Comparison of calculated and analyzed compositions

The most reliable comparison of calculated and analyzed data is for the calcite sample TBG, collected from a hydrothermal ore deposit (Tribag Mine, Ontario; Table 18, 19, Fig. 12, 13). Unlike the other samples, the water data used in the chemical calculations were collected from fluid inclusions within the calcite itself (Norman, 1977). A direct genetic relationship between the depositing water and the calcite is in place for this system.

For the geothermal samples, BR11 (Broadlands-Ohaaki, New Zealand) shows good correlation of metal concentrations in calcite between the calculated and the analyzed data. The analyzed calcite was collected from a slotted liner in the geothermal system pipes; the water samples were gathered from samples collected at weirbox (surface sampler) conditions. The initial wellhead pressure is also known, therefore the chemistry of the water before steam loss can be calculated. Similar sampling control exists for sample NT (Nigorikawa, Japan) and DV (Dixie Valley, Nevada).

The analyzed and calculated data for other geothermal samples do not correspond as well as for the above samples. The Coso Junction calcite samples (COSO 8 and 20) are finely banded and have more than one phase (Appendix A), which may represent multiple deposition periods. For this reason, it is uncertain if the water data represent the fluids that deposited the analyzed calcite. Hedenquist (personal communications, 1995) believes that water chemistry data colleted at the surface of a geothermal field can be significantly different than that at downhole conditions. A proportion of the metals in the system are depleted during flashing of the water in the wellhead, and this depleted water is most commonly used for water analysis.

Calculated compositions for the Salton Sea Scientific Drilling Project (sample SSDP) are questionable because of the extremely saline reservoir at this geothermal site (see below); the activity of aqueous species is not well understood in saline waters. The one vein calcite sample, VC2B, is from the Continental Scientific Drilling Project (CSDP), Valles Caldera, New Mexico. Data for copper, lead, and zinc are listed as less than detection limits for these particular metals; therefore, it is impossible to calculate compositions of the metals in calcite. Analyzed calcite data for sample STB (Steamboat, Nevada) was collected, yet due to lack of water chemistry at this geothermal field, no comparison between analyzed and calculated compositions is possible.

Limitations

Most obvious is the discrepancy between the measured data and the calculated data at low concentrations (Fig. 10, Table 18). Some of the measurements are more than an order of magnitude higher than expected for samples calculated to have concentrations of a particular metal at 0.01 ppm or less. Such levels in calcite are difficult to resolve using atomic absorption spectrometry (AA) because matrix interference problems raise the detection limit for most elements (Fig. 2). This problem of high calcium in solution was reduced (Fig. 7) using ion exchange chromatography (IEX); however, in order to improve the analytical accuracy, all aliquots were evaporated to increase the metal concentration. This also increased the calcium concentration; 80 to 800 ppm calcium were measured in the aliquots. This amount of calcium may cause some interference during AA analysis, especially for lead (Fig. 3).

However, the relatively high concentrations of Mg and Fe allowed us to measure these cations directly in the liquid samples, because the interference effects caused by calcium on cation analysis is less at higher cation concentrations.

A further limitation involves metal speciation with anions. For the sake of simplicity, we considered only the chloride ion in the predictive chemistry calculations. However, in hydrothermal systems with substantial amounts of sulfur, it is likely that a sulfur complex is a major transport ligand for Cu, Pb, Zn, Fe, and perhaps Mn. The sample TBG (Tribag mine, Ontario) is from a hydrothermal system, and may have been influenced by metal-HS^- complexation. There is a substantial amount of chloride in the depositing water for sample TBG (33,500 ppm); however, it is possible that HS^- formed complexes with the metals. This leads to the possibility that the amount of each metal in calcite is less than that calculated (Table 18). Therefore, the measured calcite samples should be deposited from waters with a higher concentration of total metals in solution (Table 19). If HS^-, as well as Cl^-, forms complexes with a particular metal, then less M^{2+} is available to be incorporated into calcite upon deposition. Realistically, the metals studied here form aqueous complexes with many anion species, yet the amount of data concerning complexation constants (for example, HS^-, OH^-, and HCO_3^-) forced us to tabulate somewhat elementary calculations.

Copper valence

The data for copper is inaccurate because low temperature assumptions were applied to high temperature conditions. It has been shown that copper is in the univalent state at temperatures and oxygen fugacities found in geothermal systems and ore deposits (Rose, 1976). In fact, the ratio of Cu^+:Cu^{2+} at these conditions is about 10^8; only a minimal amount of Cu^{2+} would be in the depositing water (and therefore a low concentration of copper should be incorporated into the calcite mineral lattice). However, copper was analyzed in the calcite samples; it may be that the univalent copper ion is of similar size to the calcium ion, yet Henry's Law constants and solubility products cannot be used in this case since solid solution theory is not applicable for non-divalent cations such as Cu^+.

Furthermore, there is no known case of rhombohedral copper carbonate existing in nature (Smith, 1995); therefore, theoretical data concerning solid solution chemistry of this species and calcite cannot be accurately applied to real depositing systems.

Saline water systems

For dilute waters (≤ 0.10 molar), the activity coefficients of ions can be calculated using a version of the Debye-Hückel equation (Brimhall and Crerar, 1987). In highly saline solutions, the activity of aqueous species deviates significantly from the ideal (Pitzer, 1981; Brimhall and Crerar, 1987; McKibben and Williams, 1991). Activity coefficients for ions used for the sample TBG (precipitated from a water of ionic strength at 0.4 molar) are calculated using the Davies equation (Appelo and Postma, 1993). The Davies equation is used to calculate activity coefficients only for sample TBG, as this equation has a more limited range of applicability (0.1 to 0.5 molal ionic strength). Henley, et al. (1984) suggest that the Debye-Hückel equation is relevant for solutions of ionic strength up to 9 molal. Unfortunately, the activity of neutral species cannot be taken as unity, making solid solution predictive models even more complex.

A lack of experimental data for divalent metal-chloride species (Brimhall and Crerar, 1987) led us to use of the Debye-Hückel equation (as in the computer program ION) to calculate activity coefficients for the Salton Sea geothermal field (sample SSDP). However, the decreased activity of the chloride ion in solution is one reason error occurs in solid solution calculations for the Salton Sea geothermal system (McKibben and Williams, 1989). Also, the increased importance of $CaCl_2$ as a complexing agent serves to decrease the activity of chloride. In solutions with high calcium concentrations (SSDP = 0.6 m), calcium serves as a chloride "sink" thus resulting in a decreased complexation of divalent metal ions with chloride. McKibben and Williams (1991) note the importance of Fig. 4 in Williams-Jones and Seward (1989); up to 30 percent of the chloride in solution at 300°C exists as $CaCl_2$. This would lead to a larger proportion of, for example, Pb^{2+} available for incorporation into calcite.

Geological applications

The goal of this study is to test recent theoretical data concerning solid solution chemistry; i.e., the relationship between the chemistry of a fluid to that of the minerals such fluid deposits. Newly calculated Henry's Law constants and solubility products (Smith and Jenne, in press) allow us to predict the trace level concentrations of various divalent metals in a paleowater, using the chemistry of the deposited calcite. A geological application for this concerns the paragenetic relationships in ore deposits. Calcite precipitates from fluids along with ore minerals in certain deposits, and measurements of calcite from such assemblages can lead to predictions of the ore fluid chemistry. Because calcite is ubiquitous in many deposits, analysis of multi-stage calcite may show chemical evolution of the depositing fluid. The chemical relationship between the solution and the calcite for five metals (Cu, Pb, Zn, Mg, and Fe) that can exist under equilibrium conditions is shown to rely on temperature, ionic strength of the solution, chloride concentration, and the concentration ratio between each metal and calcium in solution.

To illustrate the effect of temperature on the activity of aqueous species, the concentrations of metals calculated to be in calcite sample BR11 were modeled over a range in temperature using algorithms created for this study. If all other chemical conditions remain constant, the overall trend shows the amount of calcium incorporated into the structure of calcite is inversely related to temperature (Fig. 14), whereas the opposite is true for magnesium. These trends are controlled by the tendency of metals in solution to form chloride complexes (the simplification mentioned above), some more likely to do so at higher temperatures than others. For example, with 1000 ppm of Cl^- and 1 ppm zinc in solution, 100 times more zinc can be incorporated into calcite at 100°C than at 300°C. It follows that the amount of chloride in solution also controls the amount of metal (II) available to substitute for Ca^{2+} in the calcite structure (Fig. 15).

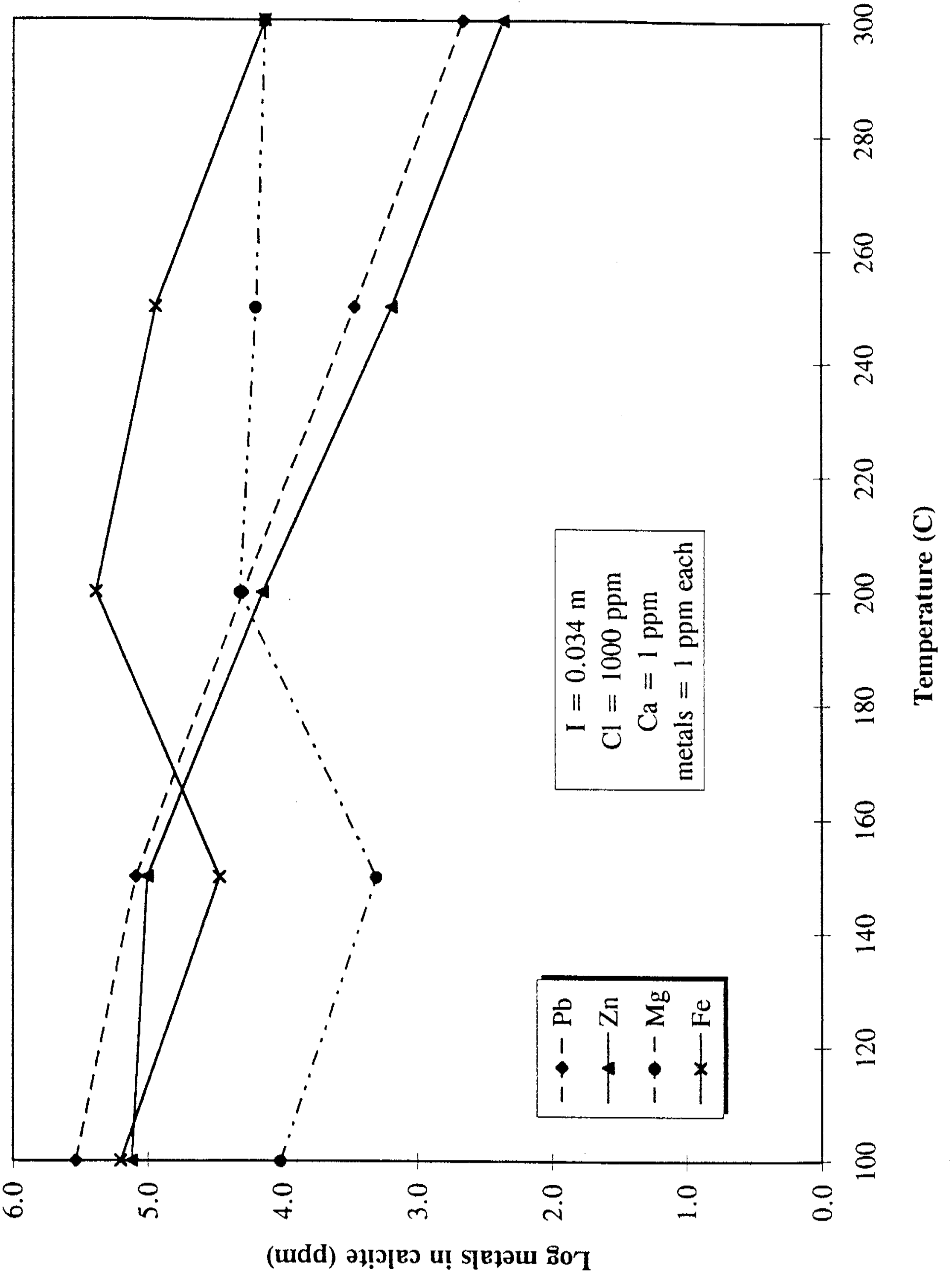

Fig. 14. Calculated concentrations of Pb, Zn, Mg, and Fe in a theoretical sample of calcite, as a function of temperature.

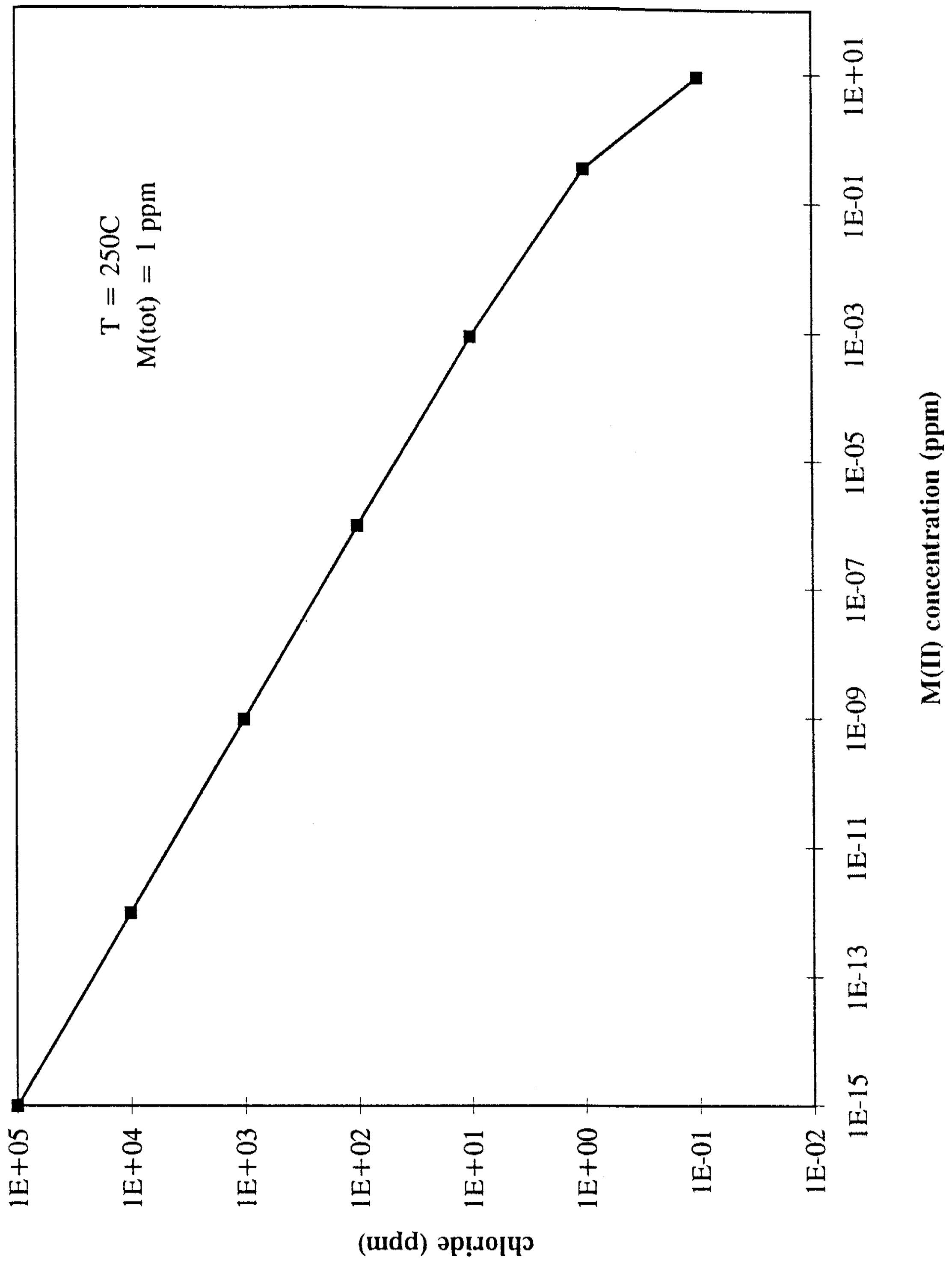

Fig. 15. Theoretical concentration of Pb, Zn, Mg, or Fe in solution (as a function of chloride concentration), assuming chloride as the only complexing agent in solution.

It is shown that as the amount of chloride in solution increases (temperature remaining constant), the metal (II) concentration will decrease and a larger fraction of the total metal in solution will exist as a chloride complex (Tsusue and Holland, 1966; Bourcier and Barnes, 1987; Heinrich and Seward, 1990).

Future work

Sampling control is the main constraint in this type of research; that is, using theory to explain real systems requires that all possible measurement errors are minimized. In this study, measurement ambiguity arose from a lack of sample control for some of the calcite locations; i.e., it is uncertain whether the calcite samples and the parent fluid are indeed genetically related. As a result, comparisons between the calculated chemistry and the measured chemistry for some calcite samples may be somewhat less than valid. In order to circumvent this problem in future studies, water samples should be collected as close as possible (both spatially and temporally) to the deposition of the calcite samples. This may be done by using downhole samplers at geothermal systems, which allow field operators to obtain a sample of the reservoir fluid.

Analytical techniques must also be carefully monitored to avoid possible error in the calcite sample measurements, specifically in the preparation of the samples for analysis. Since formic acid was used to dissolve the calcite samples, it is likely that a fraction of each of the target cations formed ionic complexes with the formate ion (Shock and Koretsky, 1995). Fortunately, the samples were acidified to a pH of 3.3 to ensure that this type of problem did not occur. In future studies, one way to keep track of possible analytical error would be to prepare blanks, in order to monitor any error additions that may occur in laboratory techniques, and to identify the steps in the analytical process which introduce the error.

CONCLUSIONS

Solid solution chemistry theory concerning divalent cation partitioning between water and calcite was successfully applied to real depositing systems. Recent theoretical data (Smith and Jenne, in press) was employed to calculate the composition of the parent fluid, using analytical data obtained from the deposited calcite. However, there are limitations that hindered these calculations; for example, it is uncertain whether equilibrium conditions existed between the calcite and the water assumed as the parent fluid. For samples collected from Coso Hydrothermal Field, the water chemistry used as the parent fluid was not the best representation of the depositing water; in fact may have been significantly different from the reservoir water.

Besides examining the data for each calcite sample, the data for each cation can be examined. Considering all the cations studied, the analytical and calculated data for Fe and Mg are comparable for most of the calcite samples, because there were high concentrations of these cations in the depositing systems (and thus, in calcite). Generally, the data for Cu, Pb, and Zn are less reliable for similar reasons: the concentrations of these cations in most of the calcite samples were quite low, which led to analytical problems. Specifically for Cu, it was shown that in the depositing systems studied here, this cation was in the univalent state (as opposed to the divalent state for the other cations). Copper is therefore less likely to replace calcium in the calcite mineral lattice.

Other limitations include the quality of the background data, especially that of cation-anion complexation. For the calculations computed in this study, the chloride ion was assumed to be the sole complexing agent in the parent fluid. This is a major simplification, since most of the cations studied here form aqueous species with a large number of anions (Garrels and Christ, 1965).

Analytical techniques were developed to measure low levels of metals in solutions of high calcium concentration. Ion exchange chromatography (IEX), a method to separate aqueous species (i.e., calcium from other divalent cations), was adapted to decrease the amount of calcium in the dissolved calcite samples, allowing for analysis of Cu, Pb, Zn, and Mn. Calcite samples were analyzed for the divalent cations listed above using atomic absorption spectrophotometry; Mg and Fe were measured directly after calcite dissolution, whereas Cu, Pb, Zn, and Mn were separated from Ca using IEX prior to AA analysis.

APPENDIX A

Sample Descriptions

Sample	Type	Location	Description	Reference
DV	fl	Dixie Valley, NV	cc scale; wt, v.fine gr (<0.5 mm), xtal	Benoit (1989); this study
COSO 8	fl	Coso Junction, CA	cc scale; gy-wh, banded (0.5 - 1 mm thick layers) xtals and crypxt, Fe ox stain on pipe-side	Moore (1994); this study
COSO 20	fl	Coso Junction, CA	cc scale; wt bld, ppt on inner pipe, rhoms on outside surface of scale.	Moore (1994); this study
NT	sf	Nigorikawa, Hokkaido, Japan	cc scale; gy-wh xtal, disagg (<2mm), ppt in 2-phase pipe.	Yoshida (1991)
BR11	sf	Broadlands/Ohaaki, New Zealand	cc scale; wh xtal, ppt on slotted liner.	Hedenquist (1990); Henley, et al. (1984)
TBG	fi	Tribag Mine, Ontario	cc min; xtal wh, samp. 7-74 (Norman, 1978).	Norman (1977)
VC2B	wb	Valles Caldera, Jemez Mtns., New Mexico	cc vein; xtal wh, CSDP corehole VC2B, 4294-4296.5 ft.	Goff (1990)
SSDP	wb	Salton, CA	cc drill; xtal wh (rhom) co-ppt with gy-grn chlorite, SSSDP well State 2-14, 3114.7-3117.0 ft.	McKibben and Williams (1989)
STB		Steamboat, NV	cc scale; wt bld, banded 1-2 cm thick.	Moore (1994)

cc: calcite
drill: drill cuttings
disagg: disaggregated
rhom: rhombic habit
min: mineral deposit
xtal: crystalline
bld: bladed habit
Fe ox: iron oxides
scale: deposited as scale in pipes
wh: white
ppt: precipitated
gy: grey
crypxt: cryptocryrstalline (very fine grained due to rapid precipitation)
fl: "flashed" (after boiling)
sf: surface water (downhole conditions calculated)
fi: fluid inclusion water (bulk analysis)
wb: collected from well bore during drilling

APPENDIX B

Analytical data for six elements, flame method

Copper

sample	mean[1] (ppm)	S.D.[2] (ppm)	R.S.D.[3](%)	C.F.[4]
DV-A2	0.08	0.02	25.0	0.52
-A3	n.d.	0.02	n.d.	0.42
COSO8-A2	0.04[5]	0.01	17.5	0.40
-A3	0.05	0.01	22.0	0.40
-B2	0.09	0.01	7.8	0.34
-B3	0.10	0.01	8.0	0.37
COSO20-A2	0.02	0.01	35.0	0.35
-A3	0.34	0.01	2.9	0.44
-B2	0.07	0.01	14.3	0.72
-B3	0.07	0.01	10.0	0.81
NT-A2	0.10	0.01	5.0	0.33
-A3	0.11	0.01	6.4	0.33
-B2	0.04	0.01	12.5	0.63
-B3	0.06	0.01	20.0	0.59
-C2	0.09	0.01	7.8	0.47
-C3	0.11	0.01	5.5	0.44
BR11-A2	0.02	0.00	n.d.	0.45
-A3	0.04	0.00	n.d.	0.29
-B2	0.01	0.01	50.0	0.34
-B3	0.04	0.02	47.0	0.33
TBG-B2	0.03	0.02	80.0	0.36
-B3	0.11	0.02	16.4	0.34
VC2B-B2	0.05	0.01	14.0	0.44
-B3	0.04	0.00	n.d.	0.36

[1] mean of 5 measurements n.d.:no data

[2] standard deviation, based on 5 consecutive measurements

[3] relative standard deviation, based on sample mean and standard deviation

[4] conversion factor for AA data, used to calculate composition in original calcite

[5] values < 0.05 ppm considered to be below AA detection limit.

Copper

sample	mean[1] (ppm)	S.D.[2] (ppm)	R.S.D.[3](%)	C.F.[4]
SSDP-A2	0.04	0.01	17.5	0.40
-A3	0.03	0.01	16.7	0.40
-B2	0.02	0.01	35.0	0.32
-B3	0.03	0.01	16.7	0.32
-D2	0.03	0.01	23.3	0.35
-D3	0.02	0.01	35.0	0.42
STB-B2	0.03	0.01	16.7	0.37
-B3	0.03	0.00	n.d.	0.29
QC[5]	0.45	0.01	1.6	1
formic[6] blank	0.00	0.00	n.d.	1
HCl[7] blank	0.00	0.00	n.d.	1
DDIW[8] blank	0.00	0.00	n.d.	1

Lead

sample	mean[1] (ppm)	S.D.[2] (ppm)	R.S.D.[3](%)	C.F.[4]
DV-A2	0.00	n.d.	n.d.	0.52
-A3	0.10	0.06	62.5	0.42
COSO8-A2	0.30	0.05	16.7	0.40
-A3	0.26	0.09	34.6	0.40
-B2	0.41	0.10	25.4	0.34
-B3	0.29	0.08	27.2	0.37
COSO20-A2	0.29	0.05	18.3	0.35
-A3	0.71	0.10	13.4	0.44
-B2	0.49	0.12	24.9	0.72
-B3	0.37	0.04	10.3	0.81
NT-A2	0.14	0.02	17.1	0.33
-A3	0.12	0.07	61.7	0.33
-B2	0.00	0.00	n.d.	0.63
-B3	0.00	0.00	n.d.	0.59
-C2	0.12	0.08	67.5	0.47
-C3	0.12	0.05	42.5	0.44
BR11-A2	0.12	0.01	5.8	0.45
-A3	0.18	0.02	11.1	0.29
-B2	0.04	0.02	37.5	0.34
-B3	0.04	0.01	32.5	0.33
TBG-B2	0.10	0.04	37.5	0.36
-B3	0.20	0.07	36.3	0.34
VC2B-B2	0.21	0.02	7.1	0.44
-B3	0.13	0.01	7.7	0.36

Lead

sample	mean[1] (ppm)	S.D.[2] (ppm)	R.S.D.[3](%)	C.F.[4]
SSDP-A2	0.09	0.02	16.7	0.40
-A3	0.07	0.02	24.3	0.40
-B2	0.11	0.03	27.3	0.32
-B3	0.08	0.02	20.0	0.32
-D2	0.10	0.02	21.0	0.35
-D3	0.08	0.02	26.3	0.42
STB-B2	0.15	0.02	12.3	0.37
-B3	0.13	0.02	10.0	0.29
QC[5]	0.51	0.05	9.2	1
formic[6] blank	0.01	0.01	n.d.	1
HCl[7] blank	0.00	0.00	n.d.	1
DDIW[8] blank	0.00	0.00	n.d.	1

Zinc

sample	mean[1] (ppm)	S.D.[2] (ppm)	R.S.D.[3](%)	C.F.[4]
DV-A2	0.02	0.01	50.0	0.52
-A3	0.03	0.01	16.7	0.42
COSO8-A2	0.17	0.01	2.9	0.40
-A3	0.15	0.01	4.7	0.40
-B2	0.18	0.01	2.8	0.34
-B3	0.16	0.01	4.4	0.37
COSO20-A2	0.05	0.01	16.0	0.35
-A3	0.41	0.01	2.9	0.44
-B2	0.16	0.01	4.4	0.72
-B3	0.14	0.00	n.d.	0.81
NT-A2	0.11	0.01	6.4	0.33
-A3	0.12	0.01	8.3	0.33
-B2	0.06	0.01	21.7	0.63
-B3	0.07	0.01	17.1	0.59
-C2	0.42	0.01	1.7	0.47
-C3	0.53	0.01	2.6	0.44
BR11-A2	0.08	0.01	8.8	0.45
-A3	0.14	0.01	5.7	0.29
-B2	0.04	0.01	17.5	0.34
-B3	0.04	0.01	17.5	0.33
TBG-B2	0.03	0.00	n.d.	0.36
-B3	0.21	0.01	3.8	0.34
VC2B-B2	0.12	0.01	5.8	0.44
-B3	0.13	0.01	3.8	0.36

Zinc

Sample	mean[1] (ppm)	S.D.[2] (ppm)	R.S.D.[3](%)	C.F.[4]
SSDP-A2	0.03	0.01	16.7	0.40
-A3	0.02	0.01	25.0	0.40
-B2	0.06	0.01	8.3	0.32
-B3	0.04	0.01	12.5	0.32
-D2	0.06	0.00	n.d.	0.35
-D3	0.03	0.01	23.3	0.42
STB-B2	0.13	0.01	5.4	0.37
-B3	0.16	0.01	8.8	0.29
QC[5]	0.53	0.01	1.32	1
formic[6] blank	0.01	0.01	70.0	1
HCl[7] blank	0.00	0.00	n.d.	1
DDIW[8] blank	0.00	0.00	n.d.	1

Magnesium

sample	mean[1] (ppm)	S.D.[2] (ppm)	R.S.D.[3](%)	C.F.[4]
DV-A	4.32	0.12	2.7	29.1
COSO8-A	7.71	0.16	2.0	505.0
-B	7.06	0.06	0.8	520.0
COSO20-A	9.26	0.16	1.7	328.9
-B	10.50	0.10	1.0	250.0
NT-A	2.92	0.12	4.2	21.6
-B	3.61	0.66	18.1	27.4
-C	3.30	0.15	4.4	21.6
BR11-A	13.63	0.14	1.0	262.5
-B	13.63	0.12	0.9	265.0
TBG-A	4.10	0.22	5.36	25.9
TBG-B	4.10	0.22	5.4	23.4
VC2B-B	4.46	0.13	2.9	24.5
SSDP-A	5.39	0.16	3.0	18.5
-B	4.89	0.21	4.4	19.2
-D	n.a.	n.a.	n.a.	n.a.
STB-A	18.79	0.34	1.8	22.7
STB-B	18.35	0.28	1.5	26.5
QC[4]	5.05	0.10	1.9	1
formic[5] blank	0.00	0.00	n.d.	1
HCl[6] blank	0.00	0.00	n.d.	1
DDIW[7] blank	0.00	0.00	n.d.	1

n.a.: not analyzed

Iron

sample	mean[1] (ppm)	S.D.[2] (ppm)	R.S.D.[3](%)	C.F.[4]
DV-A	16.25	0.24	1.4	29.1
COSO8-A	7.53	0.20	2.7	20.2
-B	7.33	0.20	2.68	20.8
COSO20-A	30.38	0.81	2.7	26.3
-B	31.90	0.71	2.2	20.0
NT-A	19.34	0.78	4.0	21.6
-B	12.00	0.34	2.8	27.4
-C	15.12	0.19	1.2	21.6
BR11-A	30.38	0.76	2.5	21.0
-B	31.64	0.37	1.2	21.2
TBG-A	5.67	0.12	2.02	25.9
TBG-B	8.04	0.12	2.0	23.4
VC2B-B	9.43	0.08	0.82	306.9
SSDP-A	20.01	0.34	1.7	92.5
-B	18.16	0.16	0.9	96.0
-D	n.a.	n.a.	n.a.	n.a.
STB-A	2.31	0.05	2.3	22.7
STB-B	2.46	0.07	2.7	26.5
QC[4]	7.41	0.14	1.2	1
formic[5] blank	0.51	0.08	16.1	1
HCl[6] blank	0.00	0.00	n.d.	1
DDIW[7] blank	0.00	0.00	n.d.	1

Manganese

sample	mean[1] (ppm)	S.D.[2] (ppm)	R.S.D.[3](%)	C.F.[4]
DV-A2	0.05	0.02	36.0	0.52
-A3	0.03	0.02	60.0	0.42
COSO8-A2	7.77	0.11	1.4	0.40
-A3	5.76	0.18	3.2	0.40
-B2	5.94	0.06	1.0	0.34
-B3	4.71	0.08	1.7	0.37
COSO20-A2	0.52	0.01	2.3	0.35
-A3	0.46	0.01	1.5	0.44
-B2	0.99	0.01	1.2	0.72
-B3	0.89	0.02	2.0	0.81
NT-A2	0.20	0.01	2.5	0.33
-A3	0.21	0.00	n.d.	0.33
-B2	0.15	0.01	3.33	0.63
-B3	0.16	0.00	n.d.	0.59
-C2	0.58	0.01	1.4	0.47
-C3	0.65	0.00	n.d.	0.44
BR11-A2	8.51	0.11	1.3	0.45
-A3	12.43	0.14	1.1	0.29
-B2	4.12	0.12	2.8	0.34
-B3	2.95	0.04	1.4	0.33
TBG-B2	3.56	0.09	2.4	0.36
-B3	0.65	0.03	4.0	0.34
VC2B-B2	2.65	0.05	1.9	0.44
-B3	2.42	0.02	0.6	0.36

Manganese

sample	mean[1] (ppm)	S.D.[2] (ppm)	R.S.D.[3](%)	C.F.[4]
SSDP-A2	17.80	0.37	2.1	0.40
-A3	12.77	0.22	1.7	0.40
-B2	24.55	0.52	2.1	0.32
-B3	18.35	0.12	0.7	0.32
-D2	30.80	0.65	2.1	0.35
-D3	18.98	0.31	1.6	0.42
STB-B2	1.86	0.02	1.2	0.37
-B3	1.42	0.03	1.8	0.29
QC[5]	0.53	0.01	2.3	1
formic[6] blank	0.02	0.01	40.0	1
HCl[7] blank	0.01	0.02	n.d.	1
DDIW[8] blank	0.00	0.01	n.d.	1

Graphite furnace method

Copper

sample	mean[1] (ppm)	R.S.D.[2](%)	C.F.[4]
NT-A2	0.027	3.5	0.33
-A3	0.030	5.9	0.33
BR11-A2	0.009	3.6	0.45
-A3	0.010	7.3	0.29
SSDP-A2	0.009	3.2	0.40
-A3	0.010	4.0	0.40
DV-A2	0.014	7.1	0.52
-A3	0.011	2.4	0.42
TBG-B2	0.005	5.8	0.36
VC2B-B2	0.011	8.1	0.44
-B3	0.015	0.9	0.36
STB-B2	0.010	2.7	0.37
STB-B3	0.018	1.2	0.29
COSO20-B2	0.022	3.1	0.35
-B3	0.023	3.7	0.44
COSO8-A2	0.011	0.8	0.40
-A3	0.014	1.9	0.40

Lead

sample	mean[1] (ppm)	R.S.D.[2](%)	C.F.[4]
NT-A2	0.015	5.9	0.33
-A3	0.012	2.7	0.33
BR11-A2	0.035	5.7	0.45
-A3	0.032	18.4	0.29
SSDP-A2	0.006	7.5	0.40
-A3	0.009	17.6	0.40
DV-A2	0.052	0.8	0.52
-A3	0.033	2.5	0.42
TBG-B2	0.005	26.2	0.36
VC2B-B2	0.016	4.5	0.44
-B3	0.039	6.5	0.36
STB-B2	0.036	1.3	0.37
STB-B3	0.024	22.3	0.29
COSO20-B2	0.256	4.7	0.35
-B3	0.230	1.3	0.44
COSO8-A2	0.055	20.2	0.40
-A3	0.062	7.7	0.40

APPENDIX C

Water chemistry data for calcite sample locations

		concentration (ppm)			
sample	location	Temp.	Cl	H_2S	I[1]
DV[2]	Dixie Valley, NV	239°C	306	n.d.	0.010
VC2B	Valles Caldera, Jemez Mtns, NM	294	4150	n.d.	0.100
COSO 8[2]	Coso Jct., CA	305	1000	n.d.	0.023
COSO 20[2]	Coso Jct., CA	305	1000	n.d.	0.047
NT	Nigorikawa, Hokkaido, Japan	237	4263	1.24	0.100
BR11	Broadlands/Ohaaki, NZ	277	1156	102	0.034
TBG	Tribag Mine, Ontario	252	33,500	n.d.	0.339
SSDP	Salton, CA	305	154,000	7.0	3.0
STB	Steamboat, NV	n.d.	n.d.	n.d.	n.d.

(continued)

	concentration (ppm)						
sample	Ca	Cu	Pb	Zn	Mg	Fe	Mn
DV[2]	5.56	0.009	0.078	0.015	0.123	0.086	0.006
COSO 8[2]	35.2	0.027	0.115	0.007	0.076	0.096	0.025
COSO 20[2]	120.7	0.065	0.215	0.020	0.038	0.318	0.083
NT[3]	16.3	0.01	0.01	0.01	2.3	0.29	n.d.
BR11	4.7	0.001	0.002	0.009	0.59	0.23	n.d.
TBG	11800	179.0	n.d.	168.0	621.0	n.d.	n.d.
VC2B	78.5	n.d.	n.d.	n.d.	0.76	15.1	3.74
SSDP	26500	6.0	95.0	506.0	36.0	1550	1390
STB	n.d.	n.d.	n.d.	n.d.	n.d.	n.d.	n.d.

[1] ionic strength of solution (mol/kg) [2] measured using AA
[3] estimated for Cu, Pb, Zn n.d.: no data
sample references are listed in Appendix A.

REFERENCES

Appelo, C.A.J. and Postma, D. 1993. Geochemistry, groundwater and pollution. A.A. Balkema, Publ., Rotterdam.

Beaty, R.D., 1978. Concepts, instrumentation, and techniques in atomic absorption spectrophotometry. The Perkin-Elmer Corp.

Berger, B.R. and Bethke, P.M. (eds.) 1985. Geology and geochemistry of epithermal systems. Reviews in Econ. Geol. v.2, Econ. Geol. Publ. Co., El Paso, TX.

Benoit, W.R. 1989. Carbonate scaling in Dixie Valley, Nevada geothermal wellbores. Geothermics 18: 41-48.

Blackburn, W.H. and Dennen, W.H. 1988. Principles of mineralogy. Wm. C. Brown, Dubuque, IA.

Blom, G. 1989. Probability and Statistics: Theory and Applications. Springer-Verlag, New York.

Bourcier, W.L. and Barnes, H.L. 1987. Ore solution chemistry VII. Stabilities of chloride and bisulfide complexes of zinc in a hydrothermal solution. Econ. Geol. 82: 1839-1863.

Brimhall, G.H. and Crerar, D.A. 1987. Ore fluids: Magmatic to supergene. Reviews in Mineralogy, v. 17, Mineralogical Society of America.

Crowley, N. and Norman, D.I. The GEOMOD hydrothermal geochemistry computer modelling code. New Mexico Institute of Mining and Technology, unpublished.

Ding, K. and Seyfried, W.E., Jr. 1992. Determination of Fe-Cl complexing in the low pressure supercritical region (NaCl fluid): Iron solubility constraints on pH of subseafloor hydrothermal fluids. Geochim. Acta 56: 3681-3692.

Garrels, R.M. and Christ, C.L. 1965. Solutions, minerals, and equilibria. Harper and Row, New York.

Goff, F., et al. 1990. The "art" of *in situ* sampling and the remarkable compositional variations in the wellbore fluid of VC-2B, Valles Caldera, New Mexico. Trans. Geotherm. Res. Council 14: 403-410.

Goff, F., et al. 1992. The Valles caldera hydrothermal systems, past and present, New Mexico, USA. Scientific Drilling 3: 181-204.

Hartley, F.R., Burgess, C., and Alcock, R.M. 1980. Solution Equilibria. Ellis Horwood, Ltd., 361 pages.

Hedenquist, J.W. 1990. The thermal and geochemical structure of the Broadlands-Ohaaki geothermal system, New Zealand. Geothermics 19: 151-185.

Heinrich, C.A. and Seward, T.M. 1990. A spectrophotometric study of aqueous iron (II) chloride complexing from 25 to 200°C. Geochim. Acta 54: 2207-2221.

Helgeson, H.C. 1969. Thermodynamics of hydrothermal systems at elevated temperatures and pressures. Am. J. Sci. 267: 729-804.

Helgeson, H.C., Kirkham, D.H., and Flowers, G.C. 1981. Theoretical prediction of the thermodynamic behavior of aqueous electrolytes at high pressures and temperatures: IV. Calculation of activity coefficients , osmotic coefficients, and apparant molal and standard and relative partial molal properties to 600°C and 5 kb. Am. J. Sci.281: 1249-1516.

Henley, R.W., Truesdell, A.H., Barton, P.B., and Whitney, J.A. (eds.) 1984. Fluid-mineral equilibria in hydrothermal systems. Reviews in Econ. Geol. v.1, Econ. Geol. Publ. Co., El Paso, TX. 267 p.

Horwitz, E.P., Chiarizia, R., Diamond, H., Gatrone, R.C., Alexandratos, S.D., Trochimczuk, A.Q., and Crick, D.W. 1993. Uptake of metal ions by a new chelating ion-exchange resin. Part 1: Acid dependencies of actinide ions. Solv. Extract. and Ion Exchange, 11.

McKibben, M.A. and Williams, A.E. 1989. Metal speciation and solubility in saline hydrothermal fluids: An empirical approach based on geothermal brine data. Econ Geol. 84: 1996-2007.

McKibben, M.A. and Williams, A.E. 1991. Metal speciation and solubility in saline hydrothermal fluids: An empirical approach based on geothermal brine data - a reply. Econ. Geol. 86: 687-689.

Moore, J. 1994. Personal communications.

Morse J.W. and Bender M.L. 1990. Partition coefficients in calcite: Examination of factors influencing the validity of experimental results and their application to natural systems. Chem. Geol. 82:256-277.

Musgrave, J.A., et. al. 1989. Selected data from Continental Drilling Core Holes VC-1 and VC-2a, Valles caldera, New Mexico. Los Alamos National Laboratory Report LA-11496-OBES, Los Alamos, New Mexico.

Musgrave, J.A. and Norman, D.I. Chemical evolution and mineralization of the Sulphur Springs hydrothermal system, Valles Caldera, New Mexico: Part I - Fluid inclusion evidence. Econ. Geol., in press.

Norman, D.I. 1977. Geology and geochemistry of the Tribag deposit, Ontario. Ph.D dissertation, University of Minnesota.

______. The computer program ION, an activity coefficient calculator for ionic species in hydrothermal systems; unpublished data.

Pitzer, K.S. 1981. Characteristics of very concentrated aqueous solutions. in D.T. Rickard and F.E. Wickman, eds. Chemistry of solutions at high temperatures and pressures. Physics and Chemistry of the Earth, v.13-14. Pergamon Press, p. 249-264.

Price, W.J. 1972. Analytical atomic absorption spectrometry. Heydon and Son, Ltd., London.

Roedder, E. 1984. Fluid inclusions. Reviews in Mineralogy. Mineralogical Society of America.

Rose, A.W. 1976. The effect of cuprous chloride complexes in the origin of red-bed copper and related deposits. Econ. Geol. 71: 1036-1048.

Seward, T.M. 1984. The formation of lead (II) chloride complexes to 300°C: A spectrophotometric study. Geochim. Acta 48: 121-134.

Shock, E.L. and Koretsky, C.M. 1995. Metal-organic complexes in geochemical processes: Estimation of standard partial molal thermodynamic properties of aqueous complexes between metal cations and monovalent organic ligands at high pressures and temperatures. Geochim. Acta 59: 1497-1532.

Smith, R.W. and Jenne, E.A. Rhombohedral carbonate solid solutions. Geochim. Acta (in press).

Smith, R.W. 1995. Personal communications.

Sûcha, L., Cadek, J., Hrabek, K., and Veselý, J. 1974. The stability of the chloro complexes of magnesium and of the alkaline earth metals at elevated temperatures. Coll. Czech. Commun. 40: 2020-2024.

Sverjensky, D.A. 1984. Prediction of Gibbs free energies of calcite-type carbonates and the equilibrium distribution of trace elements between carbonates and aqueous solutions. Geochim. Acta 48: 1127-1134.

Tsusue, A. and Holland, H.D. 1966. The coprecipitation of cations with $CaCO_3$ - III. The coprecipitation of Zn^{2+} with calcite between 50 and 250°C. Geochim. Cosmochim. Acta. 30: 439-453.

Williams-Jones, A.E. and Seward, T.M. 1989. The stability of calcium chloride pairs in aqueous solutions at temperatures between 100 and 360°C. Geochim. Acta. 53: 313-318.

Wood, S.A. 1991. Metal speciation and solubility in saline hydrothermal fluids: An empirical approach based on geothermal brine data - a discussion. Econ. Geol. 86: 685-687.

Weissberg, B.G., Browne, P.R.L., and Seward, T.M. 1979. Ore metals in active geothermal systems. in Geochemistry of hydrothermal ore deposits, 2nd edition. H.L. Barnes, ed. Wiley-Interscience, New York, p. 738-774.

Yoshida, Y. 1991. Geochemistry of the Nigorikawa geothermal system, southwest Hokkaido, Japan. Geochemical Journal 25: 203-222.

This thesis is accepted on behalf of the faculty of the Institute by the following committee:

David I. Norman

Adviser

Carl J. Popp

14 July 1995

Date